

**Zeitschrift:** Helvetica Physica Acta  
**Band:** 44 (1971)  
**Heft:** 1

**Artikel:** Coupled channel equations and the giant dipole resonance  
**Autor:** Baur, G. / Alder, K.  
**DOI:** <https://doi.org/10.5169/seals-114266>

### **Nutzungsbedingungen**

Die ETH-Bibliothek ist die Anbieterin der digitalisierten Zeitschriften auf E-Periodica. Sie besitzt keine Urheberrechte an den Zeitschriften und ist nicht verantwortlich für deren Inhalte. Die Rechte liegen in der Regel bei den Herausgebern beziehungsweise den externen Rechteinhabern. Das Veröffentlichen von Bildern in Print- und Online-Publikationen sowie auf Social Media-Kanälen oder Webseiten ist nur mit vorheriger Genehmigung der Rechteinhaber erlaubt. [Mehr erfahren](#)

### **Conditions d'utilisation**

L'ETH Library est le fournisseur des revues numérisées. Elle ne détient aucun droit d'auteur sur les revues et n'est pas responsable de leur contenu. En règle générale, les droits sont détenus par les éditeurs ou les détenteurs de droits externes. La reproduction d'images dans des publications imprimées ou en ligne ainsi que sur des canaux de médias sociaux ou des sites web n'est autorisée qu'avec l'accord préalable des détenteurs des droits. [En savoir plus](#)

### **Terms of use**

The ETH Library is the provider of the digitised journals. It does not own any copyrights to the journals and is not responsible for their content. The rights usually lie with the publishers or the external rights holders. Publishing images in print and online publications, as well as on social media channels or websites, is only permitted with the prior consent of the rights holders. [Find out more](#)

**Download PDF:** 27.11.2025

**ETH-Bibliothek Zürich, E-Periodica, <https://www.e-periodica.ch>**

# Coupled Channel Equations and the Giant Dipole Resonance

by **G. Baur** and **K. Alder**

Institute for Theoretical Physics, University of Basel

(20. VII. 70)

*Abstract.* The cross section for the ( $\gamma$ , nucleon) reaction on nuclei in the giant resonance region is calculated in a coupled channel model. 1 particle–1 hole excitations and collective surface vibrations, which are coupled to the particle degrees of freedom, are considered. It is shown that the coupled channel equations may be simplified by using the ‘external mixing’ approximation. Furthermore, the interference of E1- and E2-radiation and its influence on the angular distribution are calculated. Numerical calculations are done for the giant dipole resonance in  $C^{12}$  and  $O^{16}$  and compared with the experimental data. Contrary to the usual bound state calculations this model makes explicit predictions for the various observable quantities, such as total cross sections for photodisintegration and their angular distributions.

## I. Introduction

The main features of the giant dipole resonance for nuclei are well described in the  $1p-1h$  model [1]. (Another, equivalent approach is the collective model of Steinwedel, Jensen and Goldhaber, Teller [2].) In the first case one normally performs a shell-model calculation using bound-state wave functions (e.g. harmonic oscillator wave functions). The reaction process ( $\gamma$ ,  $N$ ) cannot be treated explicitly in this bound state model; however, the oscillator strengths are related to the cross section for  $\gamma$ -absorption. In most cases the experimentally observed fine structure is more pronounced than what one obtains from  $1p-1h$  calculations. In order to explain this fine structure the following approaches have been tried: Kamimura et al. [3] included to the usual  $1p-1h$  configurations certain  $2p-2h$  configurations. Greiner et al. [4] included in the macroscopic Steinwedel-Jensen model a coupling of the high-energy proton-neutron dipole vibration with low-energy collective vibrations and rotations. Thereby they were able to explain the fine structure of the giant dipole resonance in medium heavy and in heavy nuclei.

Buck and Hill [5] developed a coupled channel model in order to treat the giant dipole resonance as a reaction, taking into account from the outset that one has a nucleon in a continuum state. With this method one is able to calculate directly the cross section for radiative capture of nucleons by nuclei and for the time reversed process of nuclear photodisintegration. Thus one is able to give an explanation of the width of the giant dipole resonance. This method is analogous to the treatment of the atomic photoeffect. The strong residual interaction between the nucleons, however, is an additional complication, necessitating the coupling of different channels. This formalism may also be applied to elastic, inelastic and charge exchange scattering of nucleons by nuclei.

In the present work the Buck-Hill model is extended to collective surface vibrations. Numerical calculations have been done for  $C^{12}$ , where one has also observed a giant resonance based on the first excited  $2^+$  state in  $C^{12}$  by means of the reaction  $B^{11}(p, \gamma_1)C_{4.43\text{MeV}}^{12*}$ . We also develop a simplification of the coupled channel equations by using isospin invariance. Calculations are done for  $O^{16}$ , which show that the difference between neutron and proton emission is mainly due to 'external mixing'.

The observed angular distribution asymmetry about  $90^\circ$  makes it necessary to include higher multipole orders in addition to the dominant E1-radiation. We consider E2-radiation to be the most important admixture and thus we are able to explain the appearance of the angular distribution parameters  $a_1$  and  $a_3$  in the reaction  $C^{12}(\gamma, p)B^{11}$ .

## II. Giant Dipole States and Excited Giant Dipole States

Measurements of the cross sections for the reactions  $B^{11}(p, \gamma_0)C^{12}$  and  $B^{11}(p, \gamma_1)C_{4.43\text{MeV}}^{12*}$  gave an experimental indication of the coupling of the giant resonance with quadrupole surface vibrations [3] (Fig. 1a). The first excited state in  $C^{12}$  may be thought of as a collective vibrational state. Now, in order to include this excitation into the giant-resonance calculations, one might think of choosing  $2p-2h$  configurations, as has been done in [3]. But this would lead to great difficulties in the Buck-Hill model; besides, some  $3p-3h$  or  $4p-4h$  excitations might also become important. So we choose here a more phenomenological approach; following the work of Greiner et al. [4] we assume that this  $2^+$  excitation is the most important part which is coupled to the giant resonance.

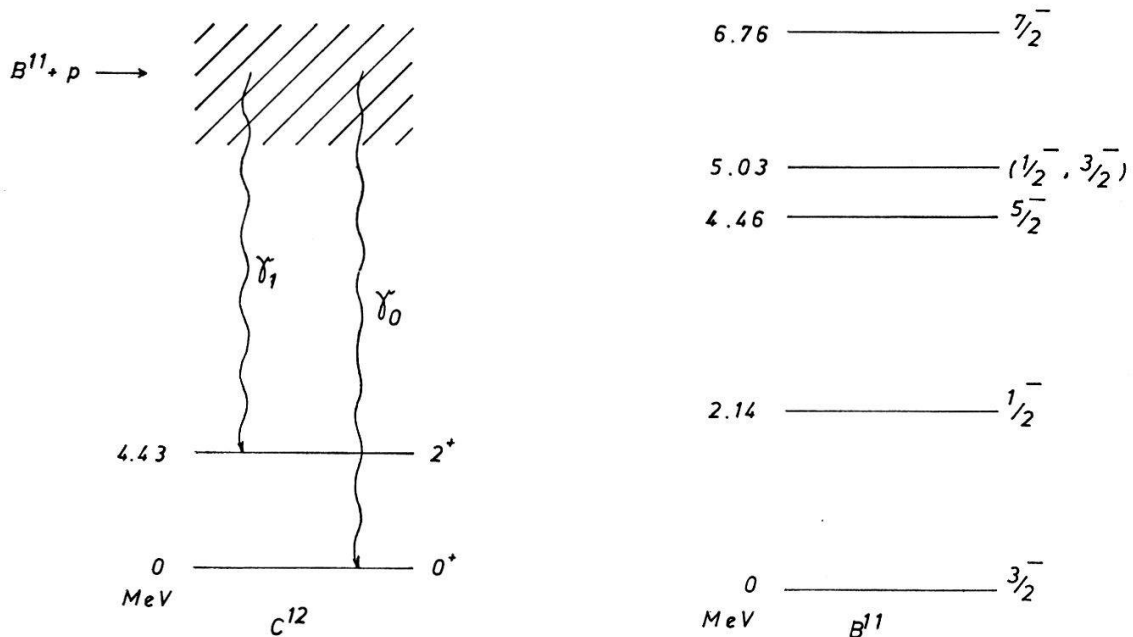


Figure 1

a. Schematic picture of the giant resonance in  $C^{12}$ , as observed in the reaction  $B^{11} + p$ .

b. Level scheme of  $B^{11}$ .

### 1. Description of the Model

The following model may in principle be applied to any even-even vibrational nuclei. As a numerical example we choose  $C^{12}$  later on.

We assume that the Hamiltonian consists of three parts:

$$H = H_p + H_{p-coll} + H_{coll}, \quad (2.1)$$

where  $H_p$  is the particle part and is given by

$$H_p = \sum_{ij} \langle i | T | j \rangle a_i^+ a_j + \frac{1}{2} \sum_{ijkl} \langle ij | V | kl \rangle a_j^+ a_i^+ a_k a_l. \quad (2.2)$$

The fermion operators  $a_i$  obey the anticommutation relations

$$\{a_i, a_j\} = \{a_i^+, a_j^+\} = 0 \quad \{a_i^+, a_j\} = \delta_{ij}. \quad (2.3)$$

The purely collective part may be written in the following form

$$H_{coll} = \hbar \omega \sum_{\mu=-2}^2 b_{\mu}^+ b_{\mu}, \quad (2.4)$$

where  $\hbar \omega$  is the energy of the first excited  $2^+$  state,  $b_{\mu}^+$  and  $b_{\mu}$  are quadrupole creation and destruction operators, satisfying the following commutation relations:

$$[b_{\mu}, b_{\mu'}] = [b_{\mu}^+, b_{\mu'}^+] = 0 \quad [b_{\mu}, b_{\mu'}^+] = \delta_{\mu\mu'}. \quad (2.5)$$

The particle-vibration coupling is written as follows:

$$H_{p-coll} = \sum_{ij\mu} \langle i | U_{\mu} | j \rangle a_i^+ a_j (b_{\mu} + (-)^{\mu} b_{-\mu}^+), \quad (2.6)$$

where  $U_{\mu}$  is given by

$$U_{\mu}(\mathbf{r}) = k(r) Y_{2\mu}(\vartheta, \varphi). \quad (2.7)$$

The function  $k(r)$  will be specified later when we have introduced the optical potential, which accounts also for this coupling, as we shall see later on.

In our model we treat the giant dipole resonance of even-even nuclei (mass number  $A$ ) as a superposition of  $1p-1h$  and collective excitations. We shall restrict ourselves to one phonon, because only one phonon seems to be established experimentally for most of the nuclei, and besides it would involve many more coupled channels without giving us more physical insight. For the ground state of the system we neglect correlations; we simply use a Slater determinant of single particle wave functions. This was found to be a good approximation by Vinh-Mau [6]. The  $2^+$  state at 4.43 MeV in  $C^{12}$  is treated as a purely collective vibrational state.

Because our Hamiltonian is invariant under rotations and the parity transformation, we decompose the total wave function  $\psi$  in the following way:

$$\psi = \sum_{J^{\pi}M} \psi_{J^{\pi}M}. \quad (2.8)$$

We shall obtain a separate Schrödinger equation for each value of the total spin  $JM$  and parity  $\pi$ . Then we make the following ansatz for our wave function with the coefficients  $C_{\alpha\beta}$ ,  $D_{\alpha\beta}^{J'}$ :

$$\begin{aligned} \psi_{J^{\pi}M} = & \sum_{\alpha\beta} C_{\alpha\beta} \langle j_{\alpha} m_{\alpha} j_{\beta} m_{\beta} | J M \rangle (-)^{\alpha} a_{\beta}^+ a_{\alpha} | 0 \rangle | 0 \rangle + \\ & \sum_{\alpha\beta M' \mu J'} D_{\alpha\beta}^{J'} \langle j_{\alpha} m_{\alpha} j_{\beta} m_{\beta} | J' M' \rangle \langle J' M' 2 \mu | J M \rangle (-)^{\alpha} a_{\beta}^+ a_{\alpha} | 0 \rangle b_{\mu}^+ | 0 \rangle. \end{aligned} \quad (2.9)$$

We use the following notation:  $|0\rangle$  is the ground state of the  $A$ -nucleon system,  $a_{\alpha}$  is the hole creation operator and  $a_{\beta}^+$  the particle creation operator. The quantum numbers of the hole are collectively denoted by  $\alpha = \varepsilon_{\alpha} l_{\alpha} j_{\alpha} m_{\alpha} - t$  where  $l_{\alpha}$  is the

orbital angular momentum,  $j_\alpha$  the total angular momentum,  $m_\alpha$  its  $z$ -component.  $-t$  is the  $z$ -component of the isospin ( $t = 1/2$  proton,  $t = -1/2$  neutron). Analogously  $\beta$  stands for  $\varepsilon_\beta l_\beta j_\beta m_\beta t$  which are the corresponding quantum numbers for the particle. The phase factor  $(-)^{\alpha} = (-)^{j_\alpha - m_\alpha}$  is introduced so that the hole state of the core nucleus transforms under rotations similarly to a particle state.  $|0\rangle$  is the phonon vacuum. Because of the explicitly inserted Clebsch-Gordan coefficients,  $C_{\alpha\beta}$  and  $D_{\alpha\beta}^{J'}$  are independent of the magnetic quantum numbers. As we have restricted ourselves to even-even nuclei we have  $J^\pi = 1^-$  for the electric dipole resonance. For the excited giant dipole resonance, as it is observed in the reaction  $B^{11}(p, \gamma_1)C^{12*}$  we must take the total spins  $1^-, 2^-, 3^-$  into account.

In practice, the sum over  $J'$  in the second term of (2.9) is replaced by the single term with  $J' = 1$ , because the quadrupole phonon will interact most strongly with the  $1^-$  giant dipole vibration. This is in accord with the purely collective model as described in [4].

## 2. Coupled Channel Equation

Using the Schrödinger equation we obtain a system of equations for the coefficients  $C_{\alpha\beta}$ ,  $D_{\alpha\beta}$ . (These coefficients depend on  $J$ , but it does not seem necessary to show this explicitly in the notation.) However, we are not directly interested in these coefficients, therefore we shall transform this system into coupled channel equations for the radial wave functions of the particle in the continuum. Putting (2.9) into the Schrödinger equation we have:

$$(0 | \langle 0 | a_\alpha^+ a_\beta (-)^{\alpha} (H - E) \psi_{J^\pi M} = 0$$

and

$$(0 | b_\mu \langle 0 | a_\alpha^+ a_\beta (-)^{\alpha} (H - E) \psi_{J^\pi M} = 0. \quad (2.10)$$

The vacuum expectation values may be calculated using the commutation and anti-commutation relations or, equivalently, the Wick theorem. So we obtain a system of linear equations known as the Tamm-Dancoff equations:

$$\begin{aligned} & C_{\alpha\beta} \langle j_\alpha m_\alpha j_\beta m_\beta | J M \rangle (\varepsilon_\beta - \varepsilon_\alpha + E_0 - E) + \sum_{\alpha'\beta'} (-)^{\alpha'+\alpha'} C_{\alpha'\beta'} \\ & \langle j_{\alpha'} m_{\alpha'} j_{\beta'} m_{\beta'} | J M \rangle \langle \beta \alpha' | V | \alpha \beta' - \beta' \alpha \rangle + \sum_{\beta' M' \mu'} D_{\alpha\beta'} \\ & \langle j_\alpha m_\alpha j_{\beta'} m_{\beta'} | J' M' \rangle \langle J' M' 2 \mu' | J M \rangle \langle \beta | U_{\mu'} | \beta' \rangle = 0, \\ & D_{\alpha\beta} \langle j_\alpha m_\alpha j_\beta m_\beta | J' M' \rangle \langle J' M' 2 \mu | J M \rangle (\varepsilon_\beta - \varepsilon_\alpha + E_0 - E + \hbar \omega) + \\ & \sum_{\alpha'\beta' M'} (-)^{\alpha+\alpha'} D_{\alpha'\beta'} \langle j_{\alpha'} m_{\alpha'} j_{\beta'} m_{\beta'} | J' M' \rangle \langle J' M' 2 \mu | J M \rangle \langle \beta \alpha' | V | \alpha \beta' - \beta' \alpha \rangle \\ & + \sum_{\beta'} C_{\alpha\beta'} \langle j_\alpha m_\alpha j_{\beta'} m_{\beta'} | J M \rangle (-)^{\mu} \langle \beta | U_{-\mu} | \beta' \rangle = 0. \end{aligned} \quad (2.11)$$

Now we want to transform this system into coupled channel equations. We first define the following single particle wave functions (solution of the Hartree-Fock equations) for bound states:

$$\phi_\alpha(\mathbf{r}) = \frac{1}{r} v_{\varepsilon_\alpha l_\alpha j_\alpha t}(\mathbf{r}) i^{l_\alpha} S_\alpha(\hat{r})$$

for continuum states:

$$\phi_{\beta}(\mathbf{r}) = \frac{1}{r} v_{\epsilon_{\beta} l_{\beta} i_{\beta} t}(\mathbf{r}) i_{\beta}^{l_{\beta}} S_{\beta}(\hat{\mathbf{r}})$$

with

$$S = \sum_{\lambda \mu} \langle l \lambda s \mu | j m \rangle Y_{l\lambda}(\hat{\mathbf{r}}) \chi_{\mu} \chi_t. \quad (2.12)$$

Then we define the following wave functions:

$$\begin{aligned} \psi_{p\alpha} &= \sum_{\epsilon_{\beta}} C_{\alpha\beta} \langle j_{\alpha} m_{\alpha} j_{\beta} m_{\beta} | J M \rangle \phi_{\beta}(\mathbf{r}) \quad (p \equiv l_{\beta} j_{\beta} t), \\ \psi_{p\alpha\mu} &= \sum_{\epsilon_{\beta}} D_{\alpha\beta} \langle j_{\alpha} m_{\alpha} j_{\beta} m_{\beta} | J' M' \rangle \langle J' M' 2 \mu | J M \rangle \phi_{\beta}(\mathbf{r}). \end{aligned} \quad (2.13)$$

Now we multiply the system (2.11) with  $\phi_{\beta}(\mathbf{r}_0)$  and sum over the excited levels of different energies  $\epsilon_{\beta}$ . This leads to terms like  $\sum_{\epsilon_{\beta}} |\phi_{\beta}(\mathbf{r}_0)\rangle \langle \phi_{\beta}(\mathbf{r}_1)|$  which we may write

by means of the completeness relation in the following way:

$$\sum_{\epsilon_{\beta}} |\phi_{\beta}(\mathbf{r}_0)\rangle \langle \phi_{\beta}(\mathbf{r}_1)| = \frac{\delta(\mathbf{r}_0 - \mathbf{r}_1)}{r_0^2} S_{\beta}(\hat{\mathbf{r}}_0) S_{\beta}(\hat{\mathbf{r}}_1) - \sum_{\epsilon_i} |\phi_i(\mathbf{r}_0)\rangle \langle \phi_i(\mathbf{r}_1)|. \quad (2.14)$$

In the future we shall neglect the contribution from the unexcited states  $i$ ; this approximation will be well justified. This sum over  $\epsilon_i$  on the right hand side of (2.14) contains only few terms, besides the overlap of the particle and hole wave function will be small because of the large energy difference.

Using the Hartree-Fock equation

$$\epsilon_{\beta} \phi_{\beta} = (T + V_{HF}) \phi_{\beta} \quad (2.15)$$

we may write (The exact form of the Hartree-Fock potential will not be used; in the actual calculation it will be replaced by a phenomenological optical potential):

$$(E_{ph} = E + \epsilon_{\alpha} - E_0),$$

$$(T + V_{HF} - E_{ph}) \psi_{p\alpha}(\mathbf{r}_0) = - \sum_{p'\alpha'} (-)^{\alpha'+\alpha'} \int d^3r_1 d^3r_2 \frac{\delta(\mathbf{r}_0 - \mathbf{r}_1)}{r_0^2}$$

$$S_{\beta}(\hat{\mathbf{r}}_0) S_{\beta}^*(\hat{\mathbf{r}}_1) \phi_{\alpha'}^*(\mathbf{r}_2) V(\mathbf{r}_1, \mathbf{r}_2) (\phi_{\alpha}(\mathbf{r}_1) \psi_{p'\alpha'}(\mathbf{r}_2) - \psi_{p'\alpha'}(\mathbf{r}_1) \phi_{\alpha}(\mathbf{r}_2))$$

$$- \sum_{M'\mu'p'} \int d^3r_1 \frac{\delta(\mathbf{r}_0 - \mathbf{r}_1)}{r_0^2} S_{\beta}(\hat{\mathbf{r}}_0) S_{\beta}^*(\hat{\mathbf{r}}_1) U_{\mu'}(\mathbf{r}_1) \psi_{p'\alpha'\mu'}(\mathbf{r}_1),$$

$$(T + V_{HF} - (E_{ph} - \hbar\omega)) \psi_{p\alpha\mu}(\mathbf{r}_0) = - \sum_{p'\alpha'} (-)^{\alpha'+\alpha'} \int d^3r_1 d^3r_2$$

$$\frac{\delta(\mathbf{r}_0 - \mathbf{r}_1)}{r_0^2} S_{\beta}(\hat{\mathbf{r}}_0) S_{\beta}^*(\hat{\mathbf{r}}_1) \phi_{\alpha'}^*(\mathbf{r}_2) V(\mathbf{r}_1, \mathbf{r}_2) (\phi_{\alpha}(\mathbf{r}_1) \psi_{p'\alpha'\mu'}(\mathbf{r}_2) -$$

$$\psi_{p'\alpha'\mu'}(\mathbf{r}_1) \phi_{\alpha}(\mathbf{r}_2)) - \sum_{p'} (-)^{\mu} \int d^3r_1 \frac{\delta(\mathbf{r}_0 - \mathbf{r}_1)}{r_0^2} S_{\beta}(\hat{\mathbf{r}}_0) S_{\beta}^*(\hat{\mathbf{r}}_1) U_{-\mu}(\mathbf{r}_1) \psi_{p'\alpha}(\mathbf{r}_1). \quad (2.16)$$

Separating the angular part of the wave function we may now obtain the radial differential equations. For this reason we define the radial functions  $f_{\alpha\beta}$  and  $g_{\alpha\beta}$ :

$$\psi_{p\alpha}(\mathbf{r}) = \frac{1}{r} f_{\alpha\beta}(r) i_{\beta}^{l_{\beta}} S_{\beta}(\hat{\mathbf{r}}) \langle j_{\alpha} m_{\alpha} j_{\beta} m_{\beta} | J M \rangle$$

with

$$f_{\alpha\beta} = \sum_{\varepsilon_\beta} C_{\alpha\beta} v_{l_\beta j_\beta t \varepsilon_\beta}(r),$$

$$\psi_{p\alpha\mu}(r) = \frac{1}{r} g_{\alpha\beta}(r) i^{l_\beta} S_\beta(\hat{r}) \langle j_\alpha m_\alpha j_\beta m_\beta | J' M' \rangle \langle J' M' 2 \mu | J M \rangle$$

with

$$g_{\alpha\beta} = \sum_{\varepsilon_\beta} D_{\alpha\beta} v_{l_\beta j_\beta t \varepsilon_\beta}(r). \quad (2.17)$$

For the residual interaction we take the following form:

$$V(r_1, r_2) = V_p \delta(r_1 - r_2) (a + b P_\sigma), \quad a + b = 1, \quad (2.18)$$

where  $P_\sigma = 1/2 (1 + \sigma_1 \cdot \sigma_2)$  is the spin-exchange operator. This  $\delta$ -function dependence avoids integral terms in our equation. This simple choice for the two-particle interaction seems justified because calculations performed so far for the giant resonance with finite range and  $\delta$ -forces have led to almost the same results.

The Hartree-Fock potential is as usual replaced by a local optical potential with a Saxon-Woods radial shape. A spin orbit, a surface absorption part and a Coulomb part have been added. For the first two, the radial shape has been assumed as the derivative of a Saxon-Woods potential

$$V_{HF} \rightarrow V_{opt} = \frac{V_0}{1 + e^{\frac{r-R}{a}}} + V_{ls} \sigma \cdot l \frac{\lambda_\pi^2}{a r} \frac{e^{\frac{r-R}{a}}}{\left(1 + e^{\frac{r-R}{a}}\right)^2} + \frac{4iW e^{\frac{r-R}{a}}}{\left(1 + e^{\frac{r-R}{a}}\right)^2} + V_{coul}. \quad (2.19)$$

Now we can also specify the function  $k(r)$ , which couples the particle motion to the vibration. A similar derivative form has also been used by Tamura [7]:

$$k(r) = \sqrt{\frac{\hbar}{2B\omega}} \frac{R}{a} V_0 \frac{e^{\frac{r-R}{a}}}{\left(1 + e^{\frac{r-R}{a}}\right)^2}. \quad (2.20)$$

The square root in (2.20)  $\sqrt{\frac{\hbar}{2B\omega}} = \frac{\beta_2}{\sqrt{5}}$  may be determined from the  $B(E2)$ -value and the energy of the  $2^+ \rightarrow 0^+$  transition [8]. We define

$$L_i^{(1)} = \frac{\hbar^2}{2M} \left( \frac{l_\beta(l_\beta + 1)}{r^2} - \frac{d^2}{dr^2} \right) + V_{opt} - E_{ph},$$

$$L_i^{(2)} = \frac{\hbar^2}{2M} \left( \frac{l_\beta(l_\beta + 1)}{r^2} - \frac{d^2}{dr^2} \right) + V_{opt} - (E_{ph} - \hbar\omega), \quad (2.21)$$

where  $M$  is the reduced mass of the system.

Now we are able to write the coupled channel equations in the following form:

$$L_i^{(1)} f_i(r) = \sum_j (A_{ij}(r) f_j(r) + B_{ij}(r) g_j(r)),$$

$$L_i^{(2)} g_i(r) = \sum_j (D_{ij}(r) f_j(r) + C_{ij}(r) g_j(r)). \quad (2.22)$$

After summing over the magnetic quantum numbers we obtain the following expressions for the coupling matrices

$$\begin{aligned}
 A_{ij} \equiv A_{\alpha\beta\alpha'\beta'} &= \frac{V_p}{4\pi} \frac{v_{l_\alpha j_\alpha i}(r) v_{l_{\alpha'} j_{\alpha'} i'}(r)}{r^2} i^{l_{\beta'} + l_\alpha - l_\beta - l_{\alpha'}} (-)^{j_\alpha + j_{\alpha'}} \\
 &\hat{j}_\alpha \hat{j}_{\alpha'} \hat{j}_\beta \hat{j}_{\beta'} \left[ (a - b \delta_{tt'}) \frac{1}{4} (1 + (-)^{J+l_\alpha+l_\beta}) (1 + (-)^{J+l_{\alpha'}+l_{\beta'}}) \right. \\
 &\left. \left( \frac{j_\alpha \ j_\beta \ J}{-1 \ 1 \ 0} \right) \left( \frac{j_{\alpha'} \ j_{\beta'} \ J}{-1 \ 1 \ 0} \right) + (b - a \delta_{tt'}) \frac{1}{4} (1 + (-)^{l_\alpha+l_{\alpha'}+l_\beta+l_{\beta'}}) \right. \\
 &\left. \left\{ \left( \frac{j_\alpha \ j_\beta \ J}{-1 \ 1 \ 0} \right) \left( \frac{j_{\alpha'} \ j_{\beta'} \ J}{-1 \ 1 \ 0} \right) + (-)^{l_\beta+l_{\beta'}+j_\beta+j_{\beta'}+1} \left( \frac{j_\alpha \ j_\beta \ J}{-1 \ -1 \ 1} \right) \left( \frac{j_{\alpha'} \ j_{\beta'} \ J}{-1 \ -1 \ 1} \right) \right\} \right],
 \end{aligned}$$

$$C_{ij} = A_{ij},$$

$$\begin{aligned}
 B_{ij} \equiv B_{\alpha\beta\alpha'\beta'} &= k(r) \sqrt{\frac{5}{4\pi}} \delta_{tt'} i^{l_{\beta'}-l_\beta} \frac{1}{2} (1 + (-)^{l_\beta+l_{\beta'}}) \\
 &(-)^{J+j_\alpha-\frac{1}{2}} \hat{j}' \hat{j}_{\beta'} \hat{j}_\beta \left( \frac{j_\beta \ j_{\beta'} \ 2}{1 \ -1 \ 0} \right) \left\{ \begin{matrix} j_\beta & J & j_\alpha \\ J' & j_{\beta'} & 2 \end{matrix} \right\},
 \end{aligned}$$

$$D_{ij} = B_{ji},$$

$$(\hat{x} \equiv \sqrt{2x+1}). \quad (2.23)$$

### 3. Calculation of the Cross Section for Radiative Capture

Now we want to calculate the cross section for the process  $(A-1) + N \rightarrow A + \gamma$ , where  $(A-1)$  is a nucleus which can be described as a pure hole state in an even-even core and  $N$  is the incoming nucleon (either a proton or a neutron). In this chapter we assume pure E1-radiation. By the theorem of detailed balance we are then able to calculate the cross section for the inverse process (photodisintegration)  $A + \gamma \rightarrow (A-1) + N$ .

The numerical integration of the system of differential equations gives us  $N$  linearly-independent solutions  $u_{pq}$ , from which we will construct the radial functions  $u_q^{(k)}(r)$  with the following asymptotic behaviour:

$$u_q^{(k)}(r) \xrightarrow[r \rightarrow \infty]{} \delta_{kq} F_q(r) + C_{kq} (G_q(r) + i F_q(r)), \quad (2.24)$$

where  $F_q$  and  $G_q$  are the regular and irregular Coulomb functions. For neutrons these functions go over into spherical Bessel and Neumann functions. In the case of closed channels (negative energy), the Whittaker and Hankel functions with imaginary arguments have an exponentially decreasing asymptotic behaviour. The incident channel is denoted by  $k$ . The solution  $u_q^{(k)}$  is obtained by linearly superposing the numerical solutions with different starting conditions:

$$u_q^{(k)} = \sum_{p=1}^N a_p^{(k)} u_{pq}. \quad (2.25)$$

Eliminating  $C_{kq}$ , we obtain a system of linear equations for the coefficients  $a_p^{(k)}$ .



Now one can calculate  $C_{kq}$  and thereby the cross sections for elastic, inelastic and charge exchange reactions of nucleons on nuclei [9].

In this work we want to calculate the cross section for  $\gamma$ -emission leaving the nucleus in its ground state or in its first vibrational state. For nuclei with  $N = Z$  we write the dipole operator for the emission of a photon with  $z$ -component  $\mu$  as follows:

$$D_\mu = D_\mu^{(0)} + D_\mu^{(1)}. \quad (2.26)$$

$D_\mu^{(0)}$  is the main term and is given by:

$$D_\mu^{(0)} = e \sum_{ij} \langle i | t_3 r Y_{1\mu}^* | j \rangle a_i^\dagger a_j. \quad (2.27)$$

$t_3$  has the eigenvalues  $+1/2$  for protons and  $-1/2$  for neutrons.  $D_\mu^{(1)}$  is the contribution from the collective motion and has been calculated by Greiner et al. [4] using the hydrodynamic model:

$$D_\mu^{(1)} = e \frac{\beta_2^2}{\sqrt{5}} \phi \sum_{\varepsilon \varepsilon' ij} \langle 2 \varepsilon 1 \varepsilon' | 1 \mu \rangle (b_\varepsilon + (-)^\varepsilon b_{-\varepsilon}^+) \langle i | t_3 r Y_{1\varepsilon'}^* | j \rangle a_i^\dagger a_j. \quad (2.28)$$

$\phi$  has been calculated in two different approximations [4]:

$\phi = -0.766$  neglecting the energy dependence of the proton density,

$\phi = -0.246$  using the adiabatic approximation.

The numerical calculations show that the influence of  $D_\mu^{(1)}$  on the total cross section is less than 10%. But the value of  $\phi$ , which is not very well known, introduces an ambiguity. So, in the final calculations this term was dropped. The following formulae include the contribution of  $D_\mu^{(1)}$  for the sake of completeness.

The initial state of the system is given by the solution of the scattering problem. Then the electromagnetic interaction is turned on causing transitions to the ground state or the excited  $2^+$ -state. We consider an incoming nucleon with the wave number  $\mathbf{k}_i$ ,  $z$ -component of spin  $\nu$ , isospin  $t$  and a target characterized by a hole with the hole quantum numbers  $j_\alpha m_\alpha l_\alpha - t$ . Then we can write the state vector of the total system as follows:

$$\begin{aligned} |z\rangle \equiv \psi_{m_\alpha \nu}^{l_\alpha j_\alpha t}(\mathbf{k}_i) &= \frac{4\pi}{k_i} \sum_{j_\beta l_\beta \lambda m_\beta J M} e^{i\sigma_{l_\beta}} Y_{l_\beta \lambda}^*(\hat{k}_i) \langle j_\alpha m_\alpha j_\beta m_\beta | J M \rangle \\ &\langle l_\beta \lambda s \nu | j_\beta m_\beta \rangle \left( \sum_{\alpha' \beta'} C_{\alpha' \beta' c_i} (-)^{\alpha'} \langle j_{\alpha'} m_{\alpha'} j_{\beta'} m_{\beta'} | J M \rangle a_{\beta'}^\dagger a_\alpha | 0 \rangle | 0 \rangle \right. \\ &\left. + \sum_{\alpha' \beta' M' \mu'} D_{\alpha' \beta' c_i} (-)^{\alpha'} \langle j_{\alpha'} m_{\alpha'} j_{\beta'} m_{\beta'} | J' M' \rangle \langle J' M' 2 \mu' | J M \rangle a_{\beta'}^\dagger a_\alpha | 0 \rangle b_\mu^+ | 0 \rangle \right), \quad (2.29) \end{aligned}$$

where  $\sigma_{l_\beta}$  is the Coulomb phase.

Now we calculate the following matrix elements:

$$B_{01\mu}^{m_\alpha \nu} = \langle 0 | D_\mu | z \rangle \text{ and } B_{2\bar{\nu}1\mu}^{m_\alpha \nu} = \langle 0 | b_{\bar{\nu}} D_\mu | z \rangle. \quad (2.30)$$

The first one describes the dipole transition to the  $0^+$  ground state of the nucleus  $A$ , the second one describes the transition to the vibrational state leaving the nucleus with  $z$ -component of angular momentum  $\bar{\nu}$ . We obtain the following result:

$$B_{01\mu}^{m_\alpha \nu} = \frac{e\sqrt{4\pi}}{k_i} \sum_{j_\beta l_\beta \lambda} e^{i\sigma_{l_\beta}} Y_{l_\beta \lambda}^*(\hat{k}_i) \langle j_\alpha m_\alpha j_\beta m_\beta | 1 \mu \rangle \langle l_\beta \lambda s \nu | j_\beta m_\beta \rangle E_1(c_i),$$

$$E_1(c_i) = E_1^{(0)}(c_i) + E_1^{(1)}(c_i).$$

$E_1^{(0)}$  is due to the term  $D_\mu^{(0)}$  of the dipole operator,  $E_1^{(1)}$  to  $D_\mu^{(1)}$ .

We have

$$E_1^{(0)}(c_i) = \sum_{\alpha'\beta'} i^{l_{\beta'}-l_{\alpha'}} t' \hat{j}_{\alpha'} \hat{j}_{\beta'} (-)^{j_{\alpha'}-\frac{1}{2}} \begin{pmatrix} j_{\alpha'} & j_{\beta'} & 1 \\ -1 & 1 & 0 \end{pmatrix} \int_0^\infty dr r v_{l_{\alpha'}j_{\alpha'}t'} f_{\alpha'\beta'c_i}, \quad (2.31)$$

$$E_1^{(1)}(c_i) = \frac{\beta_2^2 \dot{p}}{\sqrt{5}} \sum_{\alpha'\beta'} i^{l_{\beta'}-l_{\alpha'}} t' \hat{j}_{\alpha'} \hat{j}_{\beta'} (-)^{j_{\alpha'}-\frac{1}{2}} \begin{pmatrix} j_{\alpha'} & j_{\beta'} & 1 \\ -1 & 1 & 0 \end{pmatrix} \int_0^\infty dr r v_{l_{\alpha'}j_{\alpha'}t'} g_{\alpha'\beta'c_i}$$

and likewise for the  $2^+$  transition

$$B_{2\nu 1\mu}^{m_{\alpha\nu}} = \frac{e\sqrt{4\pi}}{k_i} \sum_{j_{\beta'}l_{\beta'}} e^{i\sigma l_{\beta'}} Y_{l_{\beta'}\lambda}^*(\hat{k}_i) \langle j_{\alpha} m_{\alpha} j_{\beta} m_{\beta} | JM \rangle \langle l_{\beta} \lambda s \nu | j_{\beta} m_{\beta} \rangle$$

$$(-)^M \begin{pmatrix} 1 & 2 & J \\ \mu & \bar{\nu} & -M \end{pmatrix} F_1(c_i),$$

$$F_1(c_i) = F_1^{(0)}(c_i) + F_1^{(1)}(c_i),$$

$$F_1^{(0)}(c_i) = \sum_{\alpha'\beta'} i^{l_{\beta'}-l_{\alpha'}} \hat{j}_{\alpha'} \hat{j}_{\beta'} t' (-)^{j_{\beta'}+\frac{1}{2}} \begin{pmatrix} j_{\alpha'} & j_{\beta'} & 1 \\ 1 & -1 & 0 \end{pmatrix} \int_0^\infty dr r v_{l_{\alpha'}j_{\alpha'}t'} g_{\alpha'\beta'c_i},$$

$$F_1^{(1)}(c_i) = \frac{\beta_2^2 \dot{p}}{\sqrt{5}} \sum_{\alpha'\beta'} i^{l_{\beta'}-l_{\alpha'}} \sqrt{3} \hat{j}_{\alpha'} \hat{j}_{\beta'} t' (-)^{j_{\beta'}+\frac{1}{2}} \begin{pmatrix} j_{\alpha'} & j_{\beta'} & 1 \\ 1 & -1 & 0 \end{pmatrix} \int_0^\infty dr r v_{l_{\alpha'}j_{\alpha'}t'} f_{\alpha'\beta'c_i}. \quad (2.32)$$

Using unpolarized particles and not measuring the polarizations of the outgoing particles, we may write the following expression for the differential cross section.

For the transition to the  $0^+$  state we obtain

$$\frac{d\sigma_{0^+}}{d\Omega} = \frac{16\pi}{9} \left( \frac{E_{\gamma 0}}{\hbar c} \right)^3 \frac{1}{\hbar v (2s+1) (2j_{\alpha}+1)} \sum_{m_{\alpha\nu} \mu \mu'} B_{01\mu}^{m_{\alpha\nu}} B_{01\mu'}^{m_{\alpha\nu}*} X_{1\mu}(\hat{k}_{\gamma}) X_{1\mu'}(\hat{k}_{\gamma})^*.$$

For the transition to the  $2^+$  state we obtain

$$\frac{d\sigma_{2^+}}{d\Omega} = \frac{16\pi}{9} \left( \frac{E_{\gamma 1}}{\hbar c} \right)^3 \frac{1}{\hbar v (2s+1) (2j_{\alpha}+1)} \sum_{m_{\alpha\nu} \bar{\nu} \mu \mu'} B_{2\bar{\nu}1\mu}^{m_{\alpha\nu}} B_{2\bar{\nu}1\mu'}^{m_{\alpha\nu}*} X_{1\mu}(\hat{k}_{\gamma}) X_{1\mu'}(\hat{k}_{\gamma})^*, \quad (2.33)$$

where  $X_{1\mu}$  are the vector spherical harmonics [10], defined as

$$X_{1\mu} = Y_{11\mu} = \sum_{\varepsilon\sigma} \langle 1\varepsilon 1\sigma | 1\mu \rangle Y_{1\varepsilon} e_{\sigma}. \quad (2.34)$$

Summing over the magnetic quantum numbers we obtain:

$$\frac{d\sigma_{0^+}}{d\Omega} = \frac{12e^2}{k_i^2} \left( \frac{E_{\gamma 0}}{\hbar c} \right)^3 \frac{1}{\hbar v (2s+1) (2j_{\alpha}+1)} \sum_{j_{\beta'}l_{\beta'}\bar{j}_{\beta'}l_{\beta'}Q} e^{i(\sigma l_{\beta'} - \sigma l_{\beta'})} \hat{Q}^2 \hat{j}_{\beta'} \hat{j}_{\beta'},$$

$$(-)^{j_{\alpha}-\frac{1}{2}} \begin{Bmatrix} 1 & 1 & 1 \\ 1 & 1 & Q \end{Bmatrix} \begin{pmatrix} 1 & 1 & Q \\ 0 & 0 & 0 \end{pmatrix} \begin{Bmatrix} j_{\beta} & 1 & j_{\alpha} \\ 1 & j_{\beta'} & Q \end{Bmatrix} \begin{pmatrix} j_{\beta} & j_{\beta'} & Q \\ 1 & -1 & 0 \end{pmatrix}$$

$$\frac{1}{2} (1 + (-)^{l_{\beta}+l_{\beta'}+Q}) E_1(j_{\alpha} l_{\alpha} j_{\beta} l_{\beta} t) E_1^*(j_{\alpha} l_{\alpha} j_{\beta'} l_{\beta'} t) P_Q(\cos\vartheta). \quad (2.35)$$

Using

$$\int d\Omega P_Q(\cos\vartheta) = 4\pi \delta_{Q0}$$

we obtain for the total cross section:

$$\sigma_{0^+} = \frac{16\pi e^2}{3k_i^2} \left(\frac{E_{\gamma_0}}{\hbar c}\right)^3 \frac{1}{\hbar v (2s+1)(2j_\alpha+1)} \sum_{j_\beta l_\beta} |E_1(j_\alpha l_\alpha j_\beta l_\beta t)|^2. \quad (2.36)$$

Analogously we have for the  $2^+$  transition:

$$\begin{aligned} \frac{d\sigma_{2^+}}{d\Omega} &= \frac{4e^2}{k_i^2} \left(\frac{E_{\gamma_1}}{\hbar c}\right)^0 \frac{1}{\hbar v (2s+1)(2j_\alpha+1)} \sum_{j_\beta l_\beta j_{\beta'} l_{\beta'} J \bar{J} Q} e^{i(\sigma_{l_\beta} - \sigma_{l_{\beta'}})} \hat{J} \hat{\bar{J}} (-)^{J+\bar{J}} \\ &\hat{Q} \hat{j}_\beta \hat{j}_{\beta'} (-)^{j_\alpha - 1/2} \begin{Bmatrix} 1 & 1 & 1 \\ 1 & 1 & Q \end{Bmatrix} \begin{Bmatrix} 1 & 1 & Q \\ 0 & 0 & 0 \end{Bmatrix} \begin{Bmatrix} j_\beta & J & j_\alpha \\ \bar{J} & j_{\beta'} & Q \end{Bmatrix} \begin{Bmatrix} j_\beta & j_{\beta'} & Q \\ 1 & -1 & 0 \end{Bmatrix} \begin{Bmatrix} 1 & J & 2 \\ \bar{J} & 1 & Q \end{Bmatrix} \\ &\frac{1}{2} (1 + (-)^{l_\beta + l_{\beta'} + Q}) F_1^J(j_\alpha l_\alpha j_\beta l_\beta t) F_1^{\bar{J}}(j_\alpha l_\alpha j_{\beta'} l_{\beta'} t)^* P_Q(\cos\vartheta) \end{aligned} \quad (2.37)$$

and

$$\sigma_{2^+} = \frac{16\pi e^2}{9k_i^2} \left(\frac{E_{\gamma_1}}{\hbar c}\right)^3 \frac{1}{\hbar v (2s+1)(2j_\alpha+1)} \sum_{j_\beta l_\beta J} |F_1^J(j_\alpha l_\alpha j_\beta l_\beta t)|^2. \quad (2.38)$$

Generally one may express the angular distribution in the form of a Legendre polynomial expansion:

$$\frac{d\sigma}{d\Omega} = \frac{\sigma_{total}}{4\pi} \left(1 + \sum_{\nu > 0} a_\nu P_\nu(\cos\vartheta)\right). \quad (2.39)$$

Because we have assumed pure E1-radiation only the coefficient  $a_2$  is different from 0. In the computer program we calculate  $\sigma_{total}$  and  $a_2$ . Experimentally one also observes  $a_1$  and  $a_3$  to be different from 0. This will be discussed in chapter IV.

### III. A Simplification of the Coupled Channel Equations Using Isospin Invariance

#### 1. General Remarks

Recently the coupled channel equations have been used to calculate the giant dipole resonance in light nuclei with doubly closed shells ( $C^{12}$ ,  $O^{16}$ ,  $Ca^{40}$ ) [5, 11]. These calculations have included  $1p-1h$  excitations of both neutrons and protons. Because of the different single-particle energies of proton and neutron configurations and because of the Coulomb potential the neutron and proton channels were treated separately. In the present work we couple the neutron and proton excitations to the total isospin  $T = 1$  and  $T = 0$ . In a good approximation the  $T = 0$  and  $T = 1$  channels are decoupled in the region  $r < R_m$ , where  $R_m$  is the matching radius to be specified later. By this method the numerical calculations are reduced by a factor of 4, because the computer time needed to solve the coupled channel equations is about proportional to  $N^3$  [7]. The usual matching procedure of the numerically calculated radial wave functions for  $r < R_m$  to the asymptotically correct solutions allows us to take the influence of the Coulomb energy difference and of the Coulomb potential into account exactly for  $r > R_m$ . These effects are most important in this region [12].

In the second part of this chapter we describe our method and give the necessary formulae, in the third part we discuss the results for the giant resonance in  $O^{16}$  and compare it with calculations where the  $n$ - and  $p$ -channels were treated separately. The calculations differ at most by a few percent. So the difference between  $(\gamma, n)$  and  $(\gamma, p)$  reaction cross sections are explained in a natural manner and traced back to 'external mixing'.

## 2. The Simplified System of Equations and the Matching Procedure

We start from the system of equations which may be written in matrix form in the following way:

$$\frac{d^2}{dr^2} \begin{pmatrix} f_+ \\ f_- \end{pmatrix} = \begin{pmatrix} V_{++} & V_{+-} \\ V_{-+} & V_{--} \end{pmatrix} \begin{pmatrix} f_+ \\ f_- \end{pmatrix}, \quad (3.1)$$

where  $f_{\pm}$  are 1-column matrices of the  $N$   $p$ - or  $N$   $n$ -channels ( $t = \pm 1/2$ ) and  $V_{tt'}$  are the four following  $N \times N$  coupling matrices (we do not consider collective excitations here)

$$V_{tt'}^{ij} = \delta_{ij} \delta_{tt'} \left( \frac{l_{\beta}(l_{\beta} + 1)}{r^2} + \frac{2\mu}{\hbar^2} (V_{opt}^t - E_{ph}^t) \right) + V_{BHW}^{ij}. \quad (3.2)$$

The reduced mass of the system is denoted by  $\mu$ ,  $V_{opt}^t$  is the optical potential,  $V_{BHW}^{ij}$  a coupling matrix originating from the 2-body residual interaction. We assume for this interaction a  $\delta$ -force dependence of the following kind:

$$V(\mathbf{r}_1 - \mathbf{r}_2) = V_p \delta(\mathbf{r}_1 - \mathbf{r}_2) (a + b P_{\sigma}),$$

$$a + b = 1, \quad P_{\sigma} = \frac{1}{2} (1 + \boldsymbol{\sigma}_1 \cdot \boldsymbol{\sigma}_2). \quad (3.3)$$

We have then

$$V_{BHW}^{ij} = c_{ij} [(a - b \delta_{tt'}) W_1^{ij} + (b - a \delta_{tt'}) W_2^{ij}]$$

$$c_{ij} = \frac{V_p}{4\pi} \cdot \frac{v_{l_{\alpha} i_{\alpha} t}(\mathbf{r}) v_{l_{\alpha'} i_{\alpha'} t'}(\mathbf{r})}{r^2} i^{l_{\beta'} + l_{\alpha} - l_{\beta} - l_{\alpha'}} (-)^{j_{\alpha} + i_{\alpha'}} \hat{j}_{\alpha} \hat{j}_{\alpha'} \hat{j}_{\beta} \hat{j}_{\beta'}$$

$$W_1^{ij} = \frac{1}{4} (1 + (-)^{J + l_{\alpha} + l_{\beta}}) (1 + (-)^{J + l_{\alpha'} + l_{\beta'}}) \begin{pmatrix} j_{\alpha} & j_{\beta} & J \\ -1 & 1 & 0 \end{pmatrix} \begin{pmatrix} j_{\alpha'} & j_{\beta'} & J \\ -1 & 1 & 0 \end{pmatrix}$$

$$W_2^{ij} = \frac{1}{4} (1 + (-)^{l_{\alpha} + l_{\alpha'} + l_{\beta} + l_{\beta'}}) \left\{ \begin{pmatrix} j_{\alpha} & j_{\beta} & J \\ -1 & 1 & 0 \end{pmatrix} \begin{pmatrix} j_{\alpha'} & j_{\beta'} & J \\ -1 & 1 & 0 \end{pmatrix} + \right.$$

$$\left. (-)^{l_{\beta} + l_{\beta'} + j_{\beta} + j_{\beta'} + 1} \begin{pmatrix} j_{\alpha} & j_{\beta} & J \\ -1 & -1 & 1 \end{pmatrix} \begin{pmatrix} j_{\alpha'} & j_{\beta'} & J \\ -1 & -1 & 1 \end{pmatrix} \right\}, \quad (3.4)$$

where we have used the following notation: the orbital and total angular momentum quantum numbers of the hole and the particle are denoted by  $i$  or  $j$  ( $i = \alpha \beta = l_{\alpha} l_{\beta} j_{\alpha} j_{\beta}$ ,  $j = \alpha' \beta' = l_{\alpha'} l_{\beta'} j_{\alpha'} j_{\beta'}$ ). The radial wave function of the hole is  $v_{l_{\alpha} i_{\alpha} t}(\mathbf{r})$  and  $J$  is the channel spin, which is equal to 1 in our case. Let us now write for the  $f$

$$\begin{pmatrix} f_+ \\ f_- \end{pmatrix} = \frac{1}{\sqrt{2}} \begin{pmatrix} g_0 + g_1 \\ g_0 - g_1 \end{pmatrix} \quad (3.5)$$

This corresponds to a decomposition into  $T = 0$  and  $T = 1$  channels. Assuming isospin invariance, the equations for the radial functions  $g_0$  and  $g_1$  are decoupled, i.e. we must have

$$V_{++} = V_{--}, \quad V_{+-} = V_{-+}. \quad (3.6)$$

This imposes the following conditions on our system of equations. The first one is

$$v_{l_\alpha j_\alpha \frac{1}{2}}(r) = v_{l_\alpha j_\alpha - \frac{1}{2}}(r), \quad (3.7)$$

i.e. the wave functions for the neutron and proton hole states must be the same in the same quantum state. This is fulfilled to a good approximation [13]. Anyway, present knowledge about the distribution of neutrons and protons in a nucleus does not allow us to take the differences between  $n$ - and  $p$ -wave functions into account in a reliable way. By choosing different wave functions for neutrons and protons one would at most have a fictitious improvement. Secondly the following relation must hold

$$V_{opt}^{+\frac{1}{2}} - E_{ph}^{+\frac{1}{2}} = V_{opt}^{-\frac{1}{2}} - E_{ph}^{-\frac{1}{2}}. \quad (3.8)$$

Here two effects play a role which cancel each other to a certain extent: The Coulomb displacement  $\Delta_c$  of the single particle levels and the Coulomb potential for protons which we approximate by that of a homogeneously charged sphere

$$V_c = \begin{cases} \frac{Z e^2}{r} & r \geq R \\ \frac{Z e^2}{2 R} \left( 3 - \frac{r^2}{R^2} \right) & r < R \end{cases}, \quad (3.9)$$

where  $R$  is the nuclear radius and  $Z$  the nuclear charge. Note that for  $O^{16}$  the displacement energy  $\Delta_c \approx 3.45$  MeV.

In Figure 2 we compare  $\Delta_c$  and  $V_c$  in the case of  $O^{16}$ . From this figure one can see that on the average  $\Delta_c \approx V_c$  in the region  $r < R_m$ . Thus we can decouple our system of equations into a  $T = 0$  and  $T = 1$  part. This reduces the number of coupled channels. One can also see that the difference between  $\Delta_c$  and  $V_c$  becomes important for  $r > R_m$ . However we take this effect into account in an exact way by the matching procedure, as will be outlined below.

Putting equations (3.5) into equations (3.1) we obtain the following coupled channel equations by using (3.6):

$$\begin{aligned} \frac{d^2}{dr^2} (g_0) &= (V_{++} + V_{+-}) (g_0) = (V_{diag.} + V_{ij}^{T=0}) (g_0) \\ \frac{d^2}{dr^2} (g_1) &= (V_{++} - V_{+-}) (g_1) = (V_{diag.} + V_{ij}^{T=1}) (g_1), \end{aligned} \quad (3.10)$$

where we have used the following definitions:

$$\begin{aligned} V_{ij}^{T=0} &= c_{ij} [(2a - b) W_1^{ij} + (2b - a) W_2^{ij}], \\ V_{ij}^{T=1} &= c_{ij} [ -b W_1^{ij} - a W_2^{ij} ]. \end{aligned} \quad (3.11)$$

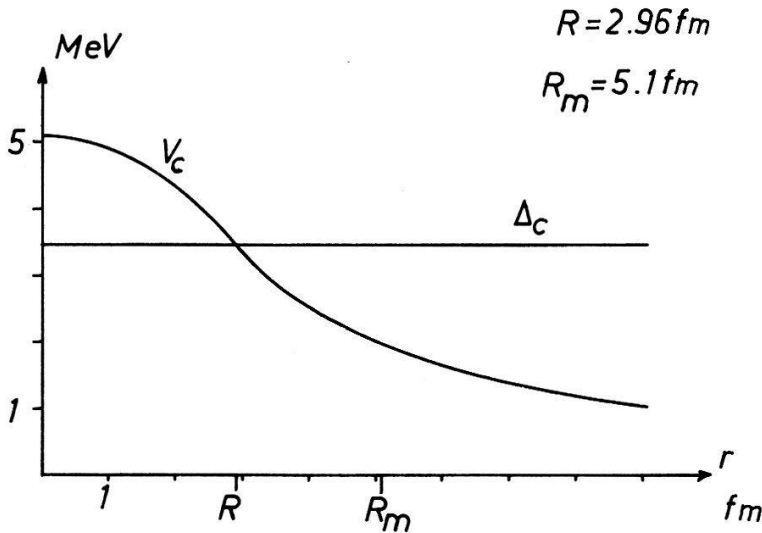


Figure 2  
Comparison of  $\Delta_c$  and  $V_c(r)$  in the case of  $O^{16}$ . The matching radius is denoted by  $R_m$ , the nuclear radius by  $R$ .

By numerical integration of the systems of differential equations (3.10) using different starting conditions, we obtain the following solutions which are regular at  $r = 0$ :

$$\begin{aligned} &\text{for } T = 1: g_1^{(i)} \\ &\text{for } T = 0: g_0^{(i)}, \end{aligned} \tag{3.12}$$

where  $i = 1, \dots, N$  is an index for the different starting conditions. Let us now form linear combinations of the following kind:

$$f_{cc_i} = \sum_{i=1}^N (a_0^{(i)} g_{0c}^{(i)} + (1 - 2\delta_{i-\frac{1}{2}}) a_1^{(i)} g_{1c}^{(i)}) \tag{3.13}$$

imposing the following boundary conditions:

$$f_{cc_i} \xrightarrow[r \rightarrow \infty]{} \delta_{cc_i} F_j + C_{cc_i} (G_j + i F_j). \tag{3.14}$$

The regular and irregular Coulomb functions are  $F_j$  and  $G_j$ . For neutrons  $F_j$  and  $G_j$  reduce to spherical Bessel- and Neumann-functions. From the matching condition of (3.13) and (3.14) at  $r = R_m$  one obtains  $4N$  linear equations for the  $4N$  unknowns  $C_{cc_i}, a_1^{(i)}, a_0^{(i)}$ . This system of linear equations may be reduced to a linear system of equations for the coefficients  $a_1^{(i)}$  and  $a_0^{(i)}$  by eliminating  $C_{cc_i}$ .

In the calculation of the dipole matrix element only the  $T = 1$  component  $g_1$  gives a contribution. The dipole operator for nuclei with an identical number of neutrons and protons (e.g.  $O^{16}$ ) is proportional to  $t_3$  and, therefore, by acting on the ground state of an even-even nucleus, the dipole operator picks out only the  $T = 1$  component. We must, however, calculate both  $T = 0$  and  $T = 1$  components for the following reason: The total wave function  $\psi$ , being a solution of the Schrödinger equation  $H\psi = E\psi$  may be formally decomposed into  $\psi = \psi_0 + \psi_1$  with  $T^2\psi_T = T(T+1)\psi_T$ . If Coulomb effects are taken into account, we have  $[H, T^2] \neq 0$ , and the Schrödinger equation does not separate into a  $T = 0$  and  $T = 1$  part. The  $T = 1$  part  $\psi_1$  by itself is not a solution of the Schrödinger equation. The  $T = 0$  part of the wave function influences the giant dipole resonance through isospin mixing with  $T = 1$ .

### 3. Results and Discussion

Numerical calculations have been performed for  $O^{16}$ . We take into account  $1p-1h$  excitations. This gives us 5 proton- and 5 neutron-channels, namely

$$(1 p_{1/2}^{-1} s_{1/2}), (1 p_{1/2}^{-1} d_{3/2}), (1 p_{3/2}^{-1} s_{1/2}), (1 p_{3/2}^{-1} d_{3/2}), (1 p_{3/2}^{-1} d_{5/2})$$

for  $n$  and  $p$  respectively.

The cross sections for the reactions  $O^{16}(\gamma, p_i) i = 0, 1$   $O^{16}(\gamma, n_i) i = 0, 1$  ( $i = 0$  transition to the ground state of the residual nucleus,  $i = 1$  transition to the  $3/2^-$ -excited state at 6.33 MeV and 6.16 MeV respectively) have been measured (for further Ref. see [5]). The cross sections for  $n$  and  $p$  emission which leave the residual nuclei in the corresponding final states are rather different from each other. The calculations, however, show that one can treat protons and neutrons symmetrically for  $r < R_m$  and explain the differences by the influence of 'external mixing'.

Figures 3–6 show the total cross sections for the four reactions which may be treated in the  $1p-1h$  model. The calculations are compared to calculations using the same set of parameter values, but treating neutrons and protons separately (10 channels). The choice of the matching radius  $R_m$  is based on the following considerations. We solve our simplified system of equations, and replace the Coulomb potential for protons by the (constant) Coulomb energy difference. Depending on the choice of  $R_m$ , this difference  $\Delta_c - V_c$  is more or less cancelled. Such calculations were performed for  $R_m = 6.1$  fm and  $R_m = 5.1$  fm. From Figure 1, one sees that the conditions for cancellation should be approximately fulfilled for these values. We obtain a slightly better agreement for  $R_m = 5.1$  fm with the calculations including all 10 channels.

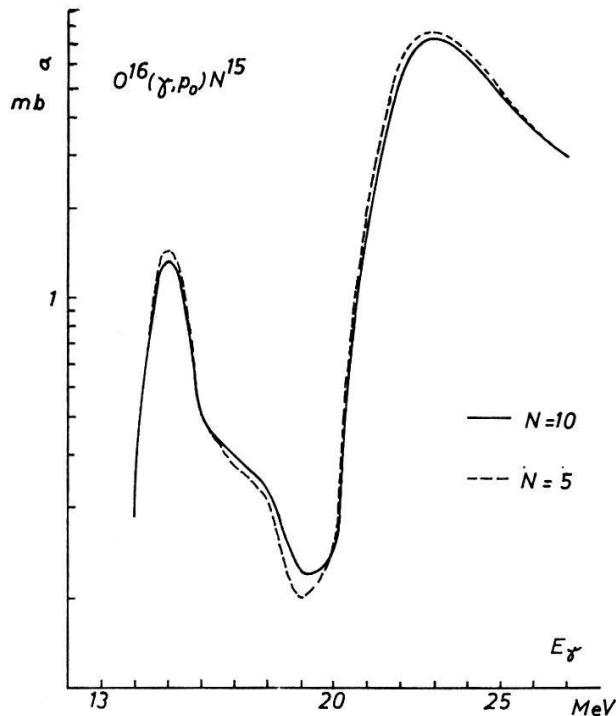


Figure 3

The total cross section for the reaction  $O^{16}(\gamma, p_0)$ . The picture shows a comparison between the calculations with  $N = 5$  and  $N = 10$  channels. The following parameter values were used throughout in Figures 3–6. For the two particle residual interaction:  $V_p = -650$  MeVfm<sup>3</sup>,  $a = 0.7$ ,  $b = 0.3$ . For the optical potential:  $V_0 = -55.0$  MeV,  $V_{1s} = -7.65$  MeV,  $R = 2.96$  fm,  $a = 0.5$  fm,  $W = 0.1 E_{proton}$ .

## IV. Numerical Results and Comparison with Experiments. Discussion

### 1. The Giant Resonance in $C^{12}$

#### a. Total Cross Sections

$C^{12}$  has been studied very often both experimentally and theoretically (for further information see Ref. [3]). The cross sections for the  $(\gamma, n)$  and  $(\gamma, p)$  processes

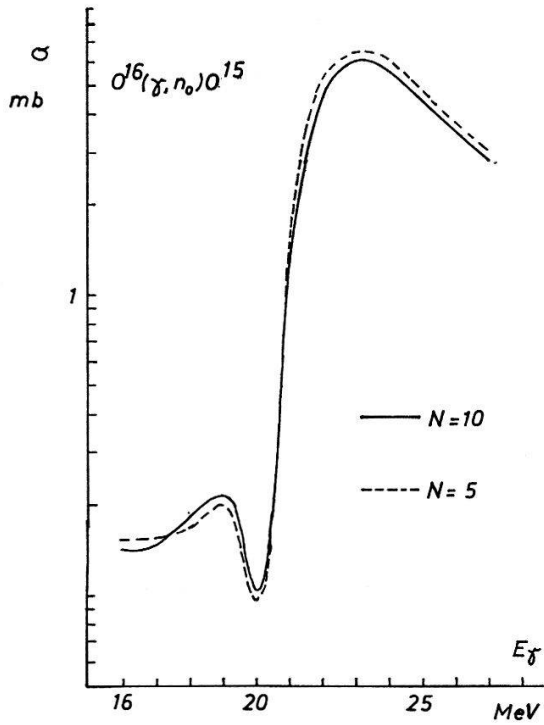


Figure 4  
The total cross section for the reaction  $O^{16}(\gamma, n_0)O^{15}$ . The same parameter values as in Figure 3 have been used.

have been measured. As final states we have considered only the ground states of  $B^{11}$  and  $C^{11}$  respectively, which are treated as pure  $p_{3/2}$  hole states. Furthermore, the cross sections for the inverse reactions  $B^{11}(p, \gamma_0)C^{12}$  and  $B^{11}(p, \gamma_1)C^{12*}$  have been measured.

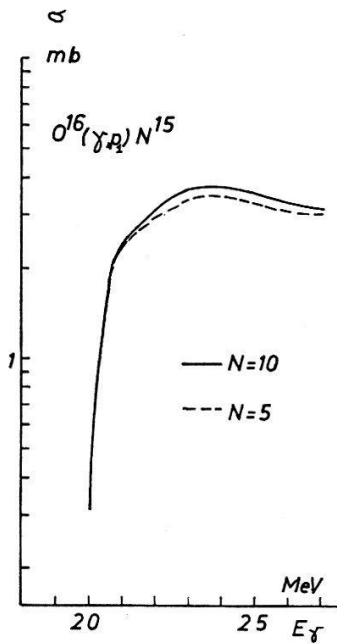


Figure 5  
The total cross section for the reaction  $O^{16}(\gamma, p_1)N^{15*}$ . The same parameter values as in Figure 3 have been used.

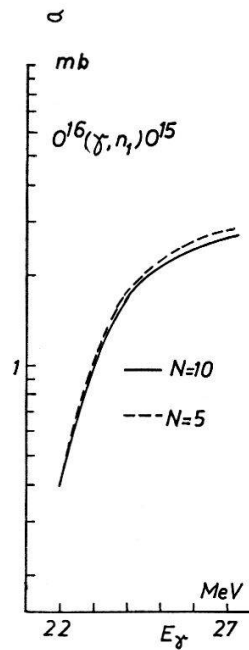


Figure 6  
The total cross section for the reaction  $O^{16}(\gamma, n_1)O^{15*}$ . The same parameter values as in Figure 3 have been used.

According to the assumed spherical-shell model, the ground state configuration for  $C^{12}$  is  $(1 s_{1/2})^2 (1 p_{3/2})^4$  for both neutrons and protons. For the giant dipole state we consider the following  $1p-1h$  excitations (for neutrons and protons):

$$(1 p_{3/2}^{-1} s_{1/2}), (1 p_{3/2}^{-1} d_{3/2}), (1 p_{3/2}^{-1} d_{5/2}), (1 s_{1/2}^{-1} p_{1/2}).$$



For the hole energies we use the following values. The  $p_{3/2}$  hole energy is 18.72 MeV for neutrons and 15.96 MeV for protons. The  $1s_{1/2}$  hole energy is 35 MeV for protons and neutrons. The  $1p_{3/2}$  hole energies have been taken from the neutron and proton separation energies of  $C^{12}$ . The  $1s_{1/2}$  hole energy for the proton has been taken from  $(p, 2p)$  experiments mentioned in Ref. [14]. The  $1s_{1/2}$  hole energy for the neutron is about the same.

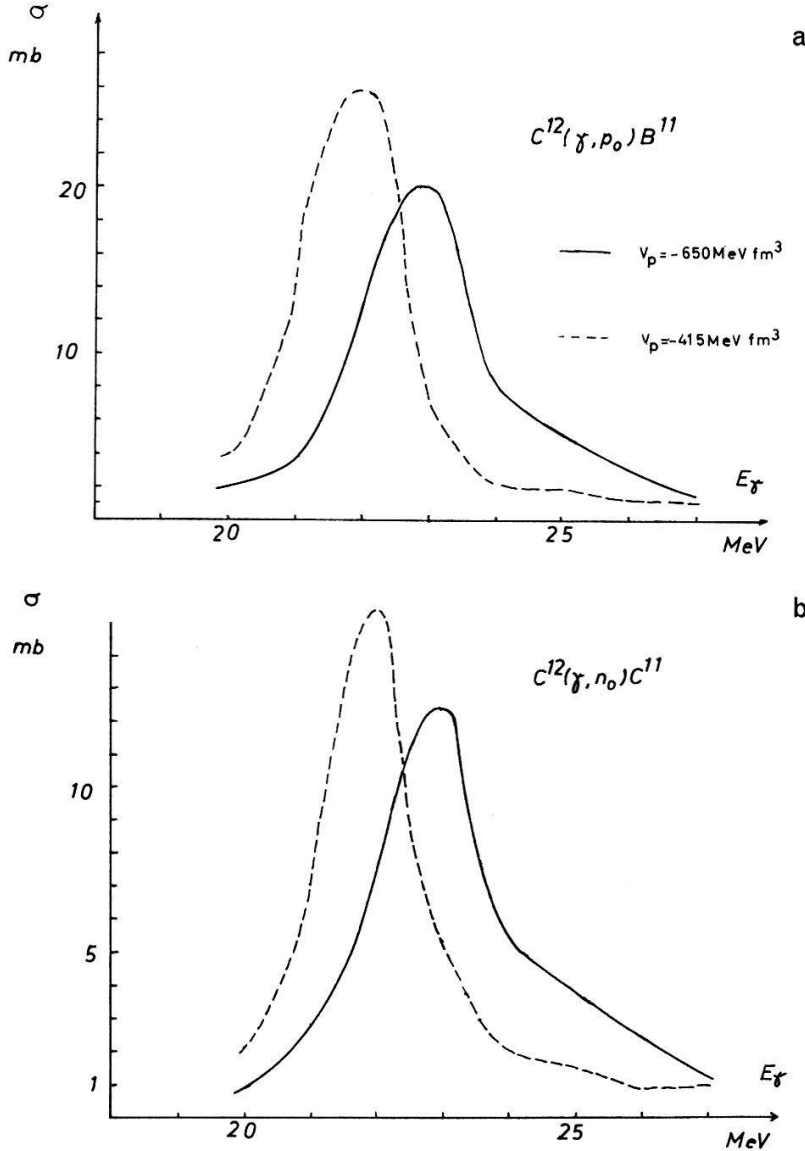


Figure 7  
The influence of the strength  $V_p$  of the two-particle interaction on the  $C^{12}(\gamma, p_0)B^{11}$  and  $C^{12}(\gamma, n_0)C^{11}$  cross section. In Figures 7–10 the following parameter values were used throughout:  $a = 0.7$ ,  $b = 0.3$ ,  $V_{1s} = -7.5$  MeV,  $R = 2.668$  fm,  $a_d = 0.425$  fm. The calculation has been performed for  $V_0 = -55$  MeV,  $\beta_2 = 0.60$  and the two different values  $V_p = -650 \text{ MeV fm}^3$  and  $V_p = -415 \text{ MeV fm}^3$ .

In order to describe the  $B^{11}(p, \gamma_1)C^{12*}$  reaction, we include a coupling of the particle degrees of freedom to the quadrupole surface vibration. As Greiner et al. [15] have shown, such a coupling may be important for light nuclei as in the case of  $C^{12}$ . One might think of extending the  $1p-1h$ -space to  $2p-2h$  configurations which is rather complicated. Besides, higher configurations such as  $3p-3h$  or  $4p-4h$  might become important. Therefore, another approach is necessary, which should be incorporated in the coupled channel method. The success of Greiner's calculations for (medium) heavy nuclei suggests that such an approach may be used for  $C^{12}$  as well. Only the lowest  $2^+$  vibration has been seen experimentally and therefore, we only take this excitation into account. The  $2^+$  state appears as a final state in the  $B^{11} + p$  reaction with about the same cross section (integrated over all energies) as the  $0^+$

ground state. The 2 parameters needed to describe this quadrupole vibration are fixed by the energy of the  $2^+$  state and the  $B(E2)$  value of the  $2^+ \rightarrow 0^+$  transition. The particle-vibration coupling term may be expressed by means of the optical potential, so that no new parameters are introduced. The Hartree-Fock potential is replaced by the local optical potential given in equation (2.19). The parameters  $V_0$ ,  $V_{1s}$ ,  $W$ ,  $R$  and  $a$  have to be considered as essentially fixed in our calculations. They were only slightly varied to obtain the best fit and to determine qualitatively the influence of a change in the parameters on the giant-resonance cross section. The strength  $V_p$  of the two particle residual interaction (see equation 2.18) is also given approximately by other experiments.

Now let us discuss the reactions  $B^{11}(\rho, \gamma_0)C^{12}$ ,  $C^{12}(\gamma, \rho_0)B^{11}$  and  $C^{12}(\gamma, n)C^{11}$ . The fine structure of the  $C^{12}$  giant resonance is not very pronounced, the calculations show good agreement with experiment. The different parameters were varied giving the following result. Figure 7 shows that an increase of the strength of the two particle interaction  $V_p$  moves the peak to higher energies, whereas an increase of the depth  $V_0$  of the Woods-Saxon potential moves the peak to lower energies, which is illustrated in Figure 8. If an absorptive part is introduced in the optical potential the cross section is lowered, especially in the region of the peaks (see Figure 9).

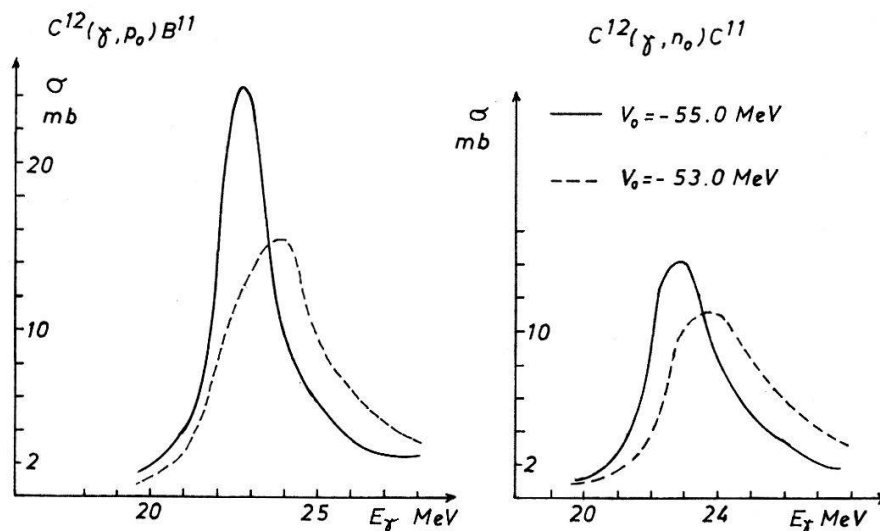


Figure 8

The influence of the depth  $V_0$  of the optical potential on the reactions  $C^{12}(\gamma, \rho)B^{11}$  and  $C^{12}(\gamma, n)C^{11}$ . The calculation has been performed with  $V_p = -415 \text{ MeVfm}^3$  and  $\beta_2 = 0.30$  and the two values of the depth parameter  $V_0 = -55 \text{ MeV}$  and  $V_0 = -53 \text{ MeV}$ .

The influence of the particle vibration coupling on the cross section is of special interest. Only in second order DWBA is such an influence obtained, and one expects therefore only a small effect. However, the coupled channel calculation of the cross section with a realistic value  $\beta_2 = 0.60$  in the case of  $C^{12}$  deviates considerably from similar calculations with  $\beta_2 = 0.0$  (see Figure 10). An increase in the strength of the particle-vibration coupling causes a decrease in the cross section for energies above the main peak ( $\sim 23 \text{ MeV}$ ). The dipole operator  $D_\mu^{(0)}$  does not change the number of phonons, but by means of the particle vibration interaction, phonons can be created. This state can, therefore, not decay into the  $C^{12}$  ground state by E1 radiation. Thus, the observed weak residual peak at  $\sim 26 \text{ MeV}$  cannot be explained in this way.

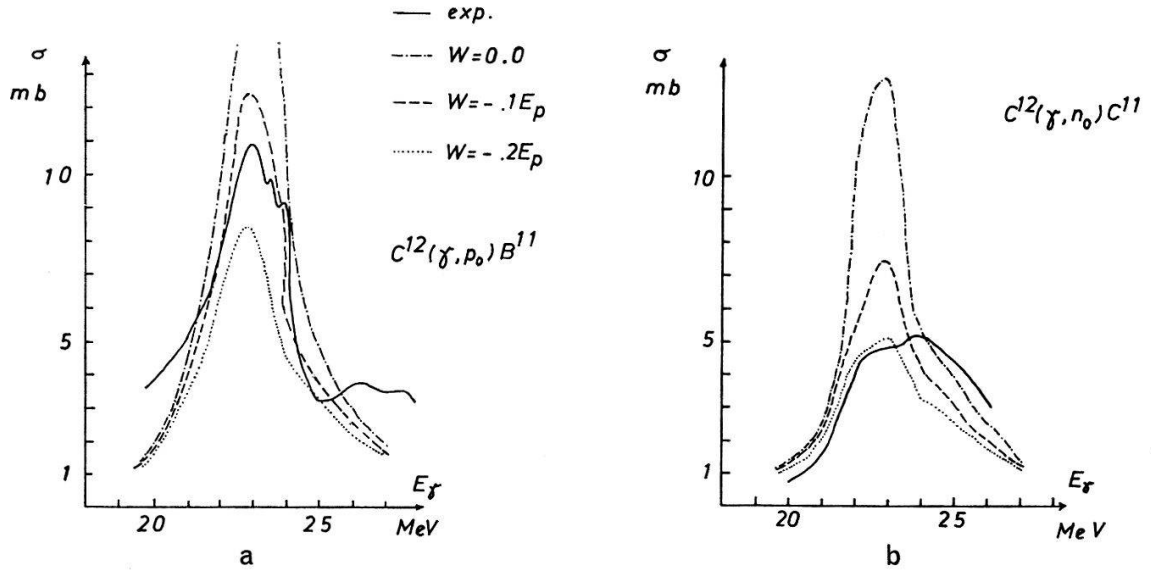


Figure 9

The influence of the absorption parameter  $W$  on the reactions  $C^{12}(\gamma, p)B^{11}$  and  $C^{12}(\gamma, n)C^{11}$ . The results are compared with experiments from Ref. [16]. The calculations have been performed with the parameters  $V_0 = -55$  MeV,  $\beta_2 = 0.60$  and the three absorption parameter  $W = 0$ ,  $W = -0.1 E_{proton}$  and  $W = -0.2 E_{proton}$ .

The reaction  $B^{11}(p, \gamma_1)C^{12*}$  allows a partial study of the giant resonance built on the 4.43 MeV level in  $C^{12}$ . Let us first give a schematic picture (see Figures 1a and 1b). We consider the ground state of  $B^{11}$  to be a  $1 p_{3/2}$  hole configuration; the excited states  $\frac{1}{2}^-$ ,  $\frac{3}{2}^-$ ,  $\frac{5}{2}^-$ ,  $\frac{7}{2}^-$  may be thought of as a phonon multiplet ( $\frac{3}{2}^- \otimes 2^+$ ) in a core excitation model. This degeneracy is removed by other interactions. The giant dipole state formed in the reaction  $C^{12} + \gamma$  contains mainly  $1p-1h$  components; therefore, one would expect the  $B^{11}$  ground state to be the main contribution to the final state. This actually happens, as may be seen by comparing the  $C^{12}(\gamma, p)$  and the  $B^{11}(p, \gamma_0)$  cross section [16]. According to the principle of detailed balance we have:

$$\frac{d\sigma}{d\Omega}(C^{12}(\gamma, p_0)B^{11}) = \frac{k_p^2}{k_\gamma^2} \frac{(2j+1)(2s+1)}{(2I_0+1)2} \frac{d\sigma}{d\Omega}(B^{11}(p, \gamma_0)C^{12}), \quad (4.1)$$

where  $k_p$  and  $k_\gamma$  are the proton and the  $\gamma$ -ray wave numbers,  $s = 1/2$  is the spin of the proton,  $j = 3/2$  the spin of  $B^{11}$  and  $I_0 = 0$  the spin of  $C^{12}$ .

Let us consider the hypothetical time reversed reaction  $C_{4.43MeV}^{12*}(\gamma, p)B_i^{11}$ , where  $i$  characterises the various final states of the residual nucleus  $B^{11}$ . This excited giant dipole resonance will contain primarily a component with a quadrupole vibration. As final states of  $B^{11}$  we expect mainly those of the phonon multiplet. The quadrupole particle coupling will be responsible for the ground state transitions. The probability of the  $B^{11}$  ground state may be estimated with the dipole sum rule (applicable also to the excited state as well as to the ground state) using the experimentally known cross section for  $B^{11}(p, \gamma_1)C^{12*}$ . Accordingly we have:

$$\int \sigma_{0+}^{E1}(E) dE = \frac{2\pi^2 e^2 \hbar}{m c} \frac{NZ}{A} (1 + 0.8x),$$

$$\int \sigma_{2+}^{E1}(E) dE = \frac{2\pi^2 e^2 \hbar}{m c} \frac{NZ}{A} (1 + 0.8x), \quad (4.2)$$

where  $\sigma_{0+}^{E1}$  is the dipole absorption from the  $C^{12}$  ground state and  $\sigma_{2+}^{E1}$  is the dipole absorption from the  $C_{4.43\text{ MeV}}^{12*}$  excited state. The parameter  $x$  is used to account for the exchange forces ( $x \sim 0.5$ ). Experimentally the dipole sum is exhausted up to 60% at 27 MeV [17]. The rest lies at higher energies where other mechanisms, such as quasi-deuteron absorption play role. We find (see Ref. [3]):

$$\int \sigma(B^{11}(p, \gamma_0)) dE \cong \int \sigma(B^{11}(p, \gamma_1)) dE \quad (4.3)$$

Applying the principle of detailed balance we obtain, apart from a kinematic factor of the order of unity,

$$\int \sigma_{0+}^{E1} dE \cong 5 \int \sigma(C^{12*}(\gamma, p_0)B^{11}) dE \quad (4.4)$$

i.e. the  $C_{4.43\text{ MeV}}^{12*}(\gamma, p_0)B^{11}$  reaction exhausts the giant dipole sum rule only to about 1/5. The other final states would be, according to our picture, excited states belonging to the phonon multiplet in  $B^{11}$  or  $C^{11}$  in the case of neutron emission. The calculations in Ref. [3] do not distinguish between these different final states.

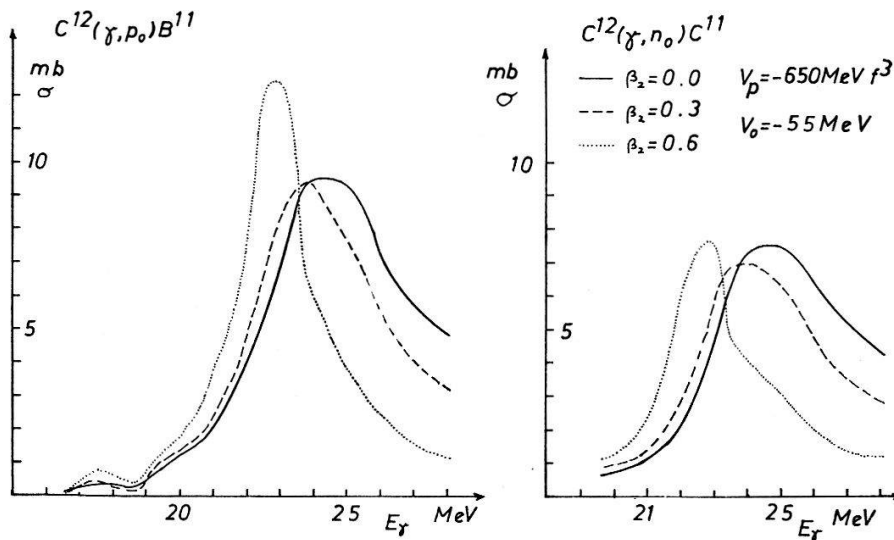


Figure 10

The influence of the vibrational parameter  $\beta_2$  on the reactions  $C^{12}(\gamma, p)B^{11}$  and  $C^{12}(\gamma, n)C^{11}$ . The calculation has been performed for the three values  $\beta_2 = 0$ ,  $\beta_2 = 0.30$  and  $\beta_2 = 0.60$ .

The total cross section for  $B^{11}(p, \gamma_1)C^{12*}$  has been calculated taking the channel spins  $1^-$ ,  $2^-$ ,  $3^-$  into account. Results for various parameter values are given in Figure 11. The cross section is too low for realistic values of  $V_p$ . However, by choosing  $V_p = 0$  and thereby neglecting the particle hole interaction one obtains a satisfactory fit to the experiment.

#### b. Angular Distribution of the $B^{11}(p, \gamma_0)$ Reaction Including E2-Radiation

The angular distribution of the  $C^{12}(\gamma, p_0)B^{11}$  (see Ref. [18]), and of the time reversed  $B^{11}(p, \gamma_0)C^{12}$  (see Ref. [19]) reaction have been measured and analysed in the form  $d\sigma/d\Omega = \sigma_0/4\pi (1 + \sum_{\nu>0} a_\nu P_\nu(\cos\theta))$ . The angular distribution parameters  $a_\nu$  are a sensitive test for the multipolarity of the  $\gamma$ -radiation and for the relative intensity and phases of the partial waves involved. The main contribution to the anisotropy

comes from  $a_2$ , which is expected, as E1-radiation is dominant. Since the distribution is asymmetric about  $90^\circ$  we require  $a_1 \neq 0$  and  $a_3 \neq 0$ . The coefficient  $a_4$  vanishes within the limits of experimental accuracy. To explain these angular distributions we must invoke interference of multipole radiation of different parities. Thus the  $a_1$  coefficient originates from either E1–M1 or E1–E2 interference or both; whereas  $a_3$  stems from E1–E2 interference. One can apply the coupled channel model for arbitrary multipole radiation. Here we consider the E2-radiation to be the most important contribution. In this model all observable quantities are completely fixed, contrary to the usual bound state calculations.

Let us first make some remarks about M1-radiation. Vinh-Mau and Brown [14] have calculated the highly excited states of  $C^{12}$  in a bound-state shell model. They found a  $1^+$  level at 16.1 MeV containing about 100% of the total M1-strength. This level consists mainly of a  $1p_{3/2}^{-1}1p_{1/2}$  configuration and is not much perturbed by the residual interaction. In order to obtain such a result, one had to assume a rather high spin-orbit splitting of 14 MeV. Since we are mainly interested in excitation energies above 16 MeV where the M1 transition strength is depleted, we neglect M1-radiation.

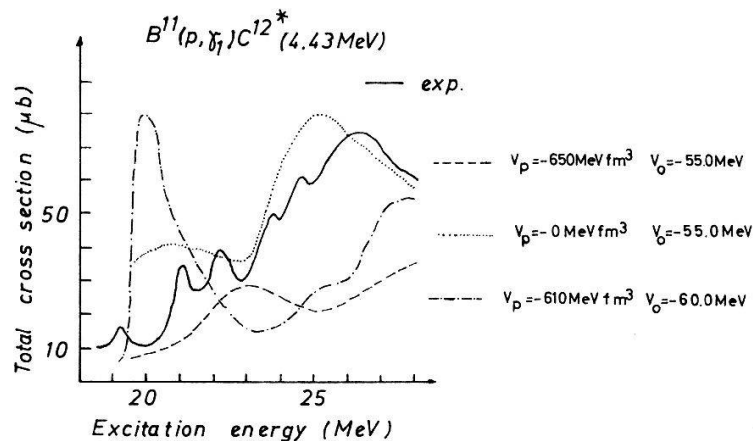


Figure 11

A comparison of the calculated total cross section for the reaction  $B^{11}(p, \gamma_1)C^{12*}$  with experiment. The experimental cross section from Ref. [3] is compared with calculated values using the following parameters.  $R = 2.67$  fm,  $a_d = 0.425$  fm,  $V_{1s} = -7.5$  MeV,  $W = 0$ ,  $a = 0.7$ ,  $b = 0.3$  and  $\beta_2 = 0.60$ . For  $V_p$  and  $V_0$  the following three combinations have been used:  $V_p = 650$  MeVfm<sup>3</sup> and  $V_0 = -55.0$  MeV,  $V_p = 0$  and  $V_0 = -55$  MeV,  $V_p = -610$  MeVfm<sup>3</sup> and  $V_0 = -60.0$  MeV.

Thus we discuss now the more important E2-radiation. Restricting ourselves to even-even nuclei, we have  $J^\pi = 2^+$  for E2 excitations. In the numerical calculation of the radial scattering functions we neglected the residual two particle interaction, thereby decoupling the system of equations. This simplification should already be a good approximation, as may be seen by a simple argument according to the schematic model of Brown and Bolsterli [1]. For repulsive forces the residual interaction shifts the collective (coherent) state to higher energies, whereas for attractive forces one obtains a collective state at lower energies. In the latter case the higher lying energy levels are not very much affected by the residual interaction. On the other hand the low lying collective level obtains a strongly enhanced transition probability from the  $2^+$  to the  $0^+$  ground state. Therefore, we expect that the residual interaction does not have an important influence in the energy region which is of interest here ( $\sim 15$ – $30$

MeV). This is quite contrary to the 1<sup>-</sup> levels in the giant resonance, where the residual interaction is decisive.

In the formalism of second quantization we write the quadrupole operator as follows:

$$Q(2\nu) = \delta_{t1/2} e \sum_{ij} \langle i | r^2 Y_{2\nu}^* | j \rangle a_i^+ a_j . \quad (4.5)$$

Now we consider the quadrupole matrix element between the excited 2<sup>+</sup> state and the ground state. The z-component of the target spin is  $m_\alpha$ ,  $\mu$  is the z-component of the spin of the projectile and  $k_i$  is its wave number. We thus have

$$Q_{m_\alpha \mu}^{l_\alpha j_\alpha t}(2\nu, \mathbf{k}_i) \equiv \langle 0 | Q(2\nu) | \psi_{m_\alpha \mu}^{l_\alpha j_\alpha t}(\mathbf{k}_i) \rangle = \frac{\sqrt{4\pi} e}{k_i} \sum_{j_\beta l_\beta \lambda} e^{i\sigma_{l_\beta}} Y_{l_\beta \lambda}^*(\hat{k}_i) \langle j_\alpha m_\alpha j_\beta m_\beta | 2\nu \rangle \langle l_\beta \lambda s \mu | j_\beta m_\beta \rangle E_2(j_\alpha l_\alpha j_\beta l_\beta t) ,$$

$$E_2(j_\alpha l_\alpha j_\beta l_\beta t) = \delta_{t1/2} i^{l_\beta - l_\alpha} \hat{j}_\alpha \hat{j}_\beta R_{\alpha\beta} (-)^{j_\beta - \frac{1}{2}} \frac{1}{2} (1 + (-)^{l_\alpha + l_\beta}) \begin{pmatrix} j_\alpha & j_\beta & 2 \\ 1 & -1 & 0 \\ 2 & 2 & 0 \end{pmatrix} , \quad (4.6)$$

where  $R_{\alpha\beta}$  denotes the radial quadrupole integral defined by

$$R_{\alpha\beta} = \int_0^\infty dr v_{l_\alpha j_\alpha t} \cdot r^2 \cdot \hat{f}_{l_\alpha j_\alpha l_\beta j_\beta t}^{2+} . \quad (4.7)$$

The radial hole wave function is denoted by  $v_{l_\alpha j_\alpha t}$  and  $\hat{f}_{l_\alpha j_\alpha l_\beta j_\beta t}^{2+}$  is the radial wave function in the continuum for the projectile. For the E1-E2 interference contribution to the differential cross section we obtain, starting from the formula for multipole radiation in [20]

$$\frac{d\sigma_{int}}{d\Omega} = \frac{4 e^2 \sqrt{5}}{k_i^2} \left( \frac{E_\gamma}{\hbar c} \right)^4 \frac{1}{\hbar v (2s+1) (2j_\alpha+1)} \text{Im} \sum_{j_\beta l_\beta j_{\beta'} l_{\beta'} Q} e^{i(\sigma_{l_\beta} - \sigma_{l_{\beta'}})} \hat{j}_\beta \hat{j}_{\beta'} Q^2 \frac{1}{2} (1 + (-)^{Q+l_\beta+l_{\beta'}}) (-)^{j_\alpha + \frac{1}{2}} \begin{pmatrix} j_\beta & j_{\beta'} & Q \\ 1 & -1 & 0 \\ 2 & 2 & 0 \end{pmatrix} \begin{pmatrix} 1 & 2 & Q \\ 0 & 0 & 0 \end{pmatrix} \begin{Bmatrix} j_\beta & 1 & j_\alpha \\ 2 & j_{\beta'} & Q \end{Bmatrix} \left\{ \begin{matrix} 1 & 1 & 1 \\ 2 & 2 & Q \end{matrix} \right\} E_1(j_\alpha l_\alpha j_\beta l_\beta t) E_2(j_\alpha l_\alpha j_{\beta'} l_{\beta'} t)^* P_Q(\cos\vartheta) , \quad (4.8)$$

where  $E_\gamma$  is the energy of the emitted  $\gamma$ -ray and  $v$  is the velocity of the projectile. This is a first order contribution of the E2-radiation. These effects have been experimentally observed. In second order, E2-radiation also contributes to the total cross section and to the angular distribution coefficients  $a_2$  and  $a_4$ . For unpolarized particles we have

$$\sigma_{total}(E2) = \frac{4\pi e^2 \kappa^5}{15 k_i^2} \frac{1}{\hbar v (2s+1) (2j_\alpha+1)} \sum_{j_\beta l_\beta} |E_2(j_\alpha l_\alpha j_\beta l_\beta t)|^2 , \quad (4.9)$$

where  $\kappa = E_\gamma / \hbar c$ . Similarly we obtain for  $a_2(\text{E}2)$  and  $a_4(\text{E}2)$

$$a_Q(\text{E}2) = \frac{5 \kappa^2}{4 \sum_{j_\beta l_\beta} |E_1(j_\alpha l_\alpha j_\beta l_\beta t)|^2} \sum_{j_{\beta'} l_{\beta'}} e^{i(\sigma_{l_\beta} - \sigma_{l_{\beta'}})} \bar{G}_{j_\beta l_\beta j_{\beta'} l_{\beta'} i_\alpha}^{-Q} E_2(j_\alpha l_\alpha j_\beta l_\beta t) E_2(j_\alpha l_\alpha j_{\beta'} l_{\beta'} t)^* \quad (4.10)$$

with

$$\bar{G}_{j_\beta l_\beta j_{\beta'} l_{\beta'} i_\alpha}^{-Q} = \hat{j}_\beta \hat{j}_{\beta'} \hat{Q}^2 \begin{pmatrix} 2 & 2 & Q \\ 0 & 0 & 0 \end{pmatrix} \begin{Bmatrix} j_\beta & 2 & j_\alpha \\ 2 & j_{\beta'} & Q \end{Bmatrix} \begin{pmatrix} j_\beta & j_{\beta'} & Q \\ 1 & -1 & 0 \\ -\frac{1}{2} & -\frac{1}{2} & 0 \end{pmatrix} \begin{Bmatrix} 2 & 2 & 1 \\ 2 & 2 & Q \end{Bmatrix} .$$

The total coefficients are thus given by

$$a_2^{\text{total}} = a_2(\text{E}1) + a_2(\text{E}2), \quad a_4^{\text{total}} = a_4(\text{E}2).$$

In Figures 12, 13, 14 the results of our calculations are given for the coefficients  $a_1$ ,  $a_2$  and  $a_3$ . In the present model the relative phases and intensities of the partial waves, on which the angular distribution coefficients depend, are explicitly determined. We now want to give a qualitative discussion of the situation.

Let  $x_{lj}$  be the dipole matrixelement for the incoming partial wave with orbital and total angular momentum  $l, j$ , normalized in the following way:

$$|x_{2\ 2/5}|^2 + |x_{2\ 2/3}|^2 + |x_{0\ 1/2}|^2 = 1. \quad (4.11)$$

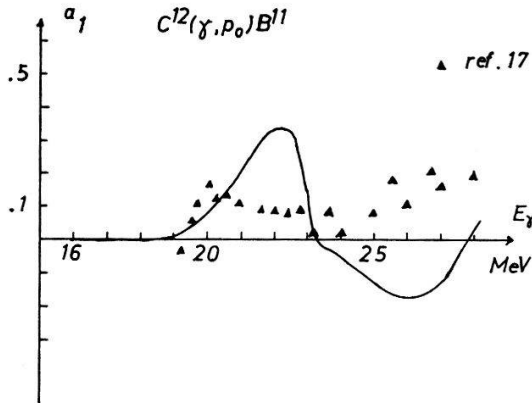


Figure 12  
The angular distribution parameter  $a_1$  for the reaction  $\text{C}^{12}(\gamma, p_0)\text{B}^{11}$ . The parameters mentioned in Figure 7 and  $V_p = -650 \text{ MeVfm}^3$  have been used in all calculations from Figures 12–15. The experimental data were taken from Refs. [17] and [18].

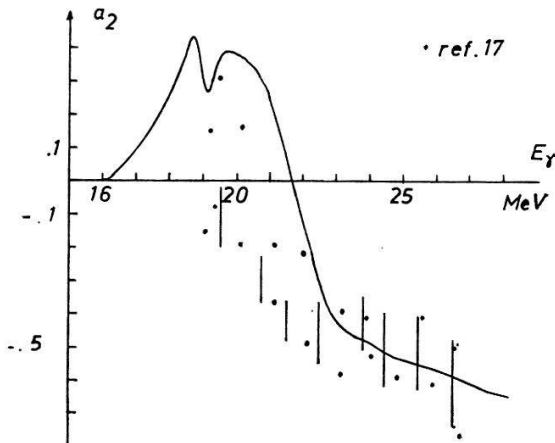


Figure 13  
The angular distribution parameter  $a_2$  for the reaction  $\text{C}^{12}(\gamma, p_0)\text{B}^{11}$ . Only E1 radiation has been taken into account.

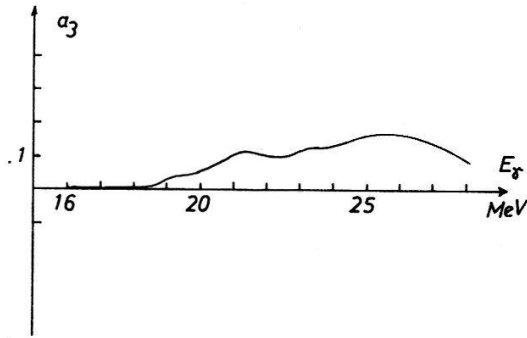


Figure 14  
The angular distribution parameter  $a_3$  for the reaction  $C^{12}(\gamma, p_0)B^{11}$ .

We obtain from (2.35) and (2.36) setting  $j_\alpha = 3/2$  and evaluating the 3  $j$ -symbols explicitly

$$\begin{aligned}
 a_2(E1) = & -\frac{2}{5} |x_{5/2}|^2 - \frac{3}{5} \operatorname{Re}(x_{5/2} x_{3/2}^*) + \frac{3}{\sqrt{5}} \operatorname{Re}(x_{5/2} x_{1/2}^*) \\
 & + \frac{2}{5} |x_{3/2}|^2 + \frac{1}{\sqrt{5}} \operatorname{Re}(x_{3/2} x_{1/2}^*) .
 \end{aligned} \quad (4.12)$$

This E1-contribution is always much larger than the corresponding E2-part. In [18] the intensities of the partial waves have been taken from particle-hole calculations and the relative phases have been fitted to the experiments. Thus all observable quantities are determined by the model. In Table I some results are compared with the results of Ref. [18]:

Table I  
Relative intensities of different partial waves compared with the results of Ref. [18]

	20–23 MeV [18]	21.7 MeV now	24–27 MeV [18]	25.9 MeV now
$q_+^2 =  x_{2\ 5/2} ^2$	91.7%	84	73.7	81
$q_0^2 =  x_{2\ 3/2} ^2$	6.8	15	12.9	18
$q_-^2 =  x_{0\ 1/2} ^2$	1.5	1	13.4	1

From this table one sees that the  $d_{5/2}$ -partial wave gives the main contribution. A pure  $d_{5/2}$ -partial wave would yield  $a_2 = -0.4$ . Thus qualitatively the following picture emerges for the different  $\gamma$ -energies.

For an energy of  $E_\gamma = 28$  MeV the  $d_{5/2}$ -contribution dominates, but we have also an appreciable negative term from the  $d_{5/2}$ - $s_{1/2}$  interference, while for  $E_\gamma = 23.8$  MeV the  $d_{5/2}$ -contribution again dominates, but because of the phase difference the  $d_{5/2}$  and  $s_{1/2}$  partial waves do not interfere. For  $E_\gamma = 19.7$  MeV the  $s_{1/2}$  partial wave dominates, but still gives rise to  $a_2 \neq 0$  due to the interference term with the  $d_{5/2}$ -partial wave.

We try to explain the occurrence of  $a_1$  and  $a_3$  by an interference of the dominant E1-with E2-radiation, neglecting the contribution of M1-radiation (which cannot contribute to  $a_3$ ). The effects of E2-radiation show up most clearly in  $a_1$  and  $a_3$ . The total cross section  $\sigma_{total}(E2)$  is always found to be smaller than 1% of the total E1 cross section. Similarly, the E2-parts of  $a_2$  and  $a_4$  have been calculated up to a  $\gamma$ -energy of 27 MeV. They are illustrated in Figure 15. It is seen that the coefficients rise with energy and that  $a_4$  is always  $< 0.02$ , while  $a_2 < 0.03$ . The experimental data



are too inaccurate for a comparison;  $a_4 \sim 0$  is consistent with the experiment. Also  $a_2$  is completely dominated by the E1-part, and it is justified to neglect the E2-part.

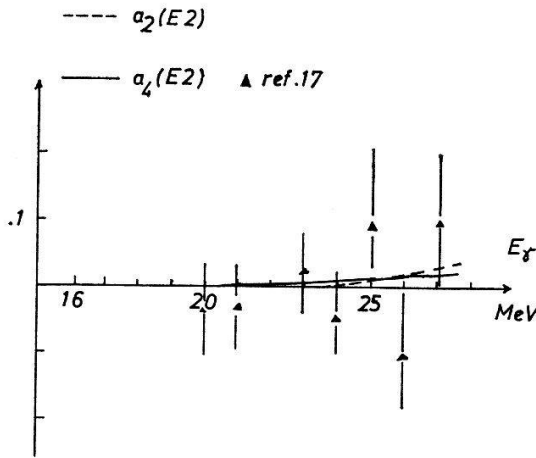


Figure 15  
The contribution to the angular distribution parameters  $a_2$  and  $a_4$  for the reaction  $C^{12}(\gamma, p_0)B^{11}$  due to E2 radiation.

In our crude model we are thus able to reproduce the order of magnitude of the observed coefficients. However, there are conflicting experimental results for the coefficient  $a_3$ , which have been obtained by different experimental methods. The authors of [18] studied the angular distribution of protons from the  $C^{12}(\gamma, p)$  reaction, using bremsstrahlung  $\gamma$ -rays. Hanna et al. [19] studied the angular distribution of the photons in the time reversed process  $B^{11}(p, \gamma)C^{12}$ . Our calculations favour  $a_3 > 0$ , as it was obtained by the authors of [19]. However, the experiments in [18] yielded  $a_3 < 0$  for the entire energy range considered.

Many different partial waves may contribute to  $a_1$  and  $a_3$ . In our calculations of the E2-radiation we have a dominant  $f_{7/2}$ -part. However, the angular distribution coefficients depend also on the relative phases between the E1- and E2-matrix elements and other partial waves become important. The important terms for  $E_\gamma = 25.4$  MeV are presented in Table II. The signs of the corresponding terms are indicated.

Table II

The important partial waves for the angular distribution coefficients  $a_1$  and  $a_3$  at  $E_\gamma = 25.4$  MeV. The signs of the corresponding terms are indicated.

$a_1$ :	$a_3$ :
$E_1(d_{5/2}) E_2(p_{3/2})^* +$	$E_1(d_{5/2}) E_2(p_{1/2})^* -$
$E_1(d_{5/2}) E_2(f_{7/2})^* -$	$E_1(d_{5/2}) E_2(p_{3/2})^* -$
$E_1(s_{1/2}) E_2(p_{1/2})^* +$	$E_1(d_{5/2}) E_2(f_{7/2})^* +$
$E_1(s_{1/2}) E_2(p_{3/2})^* +$	$E_1(s_{1/2}) E_2(f_{7/2})^* +$

By slightly changing the  $f_{7/2}$ -contribution, one can appreciably change  $a_1$  and  $a_3$ . By using different values for the  $l \cdot s$  potential or the residual interaction, the  $f_{7/2}$ -part may be suppressed in order to obtain negative values for  $a_3$ , as have been observed in Ref. [18]. The assumed model seems basically correct and accounts for the main feature. Of course, it could be improved by taking the residual interaction into account, but this would lead to a much greater numerical effort and would not alter the situation significantly. One could also argue that the  $2p-2h$  ( $1 \hbar \omega$ ) configurations should be included. These lie in the same energy region as the  $1p-1h$  ( $2 \hbar \omega$ ) energies used here. However, it seems too difficult to carry through such a programme.

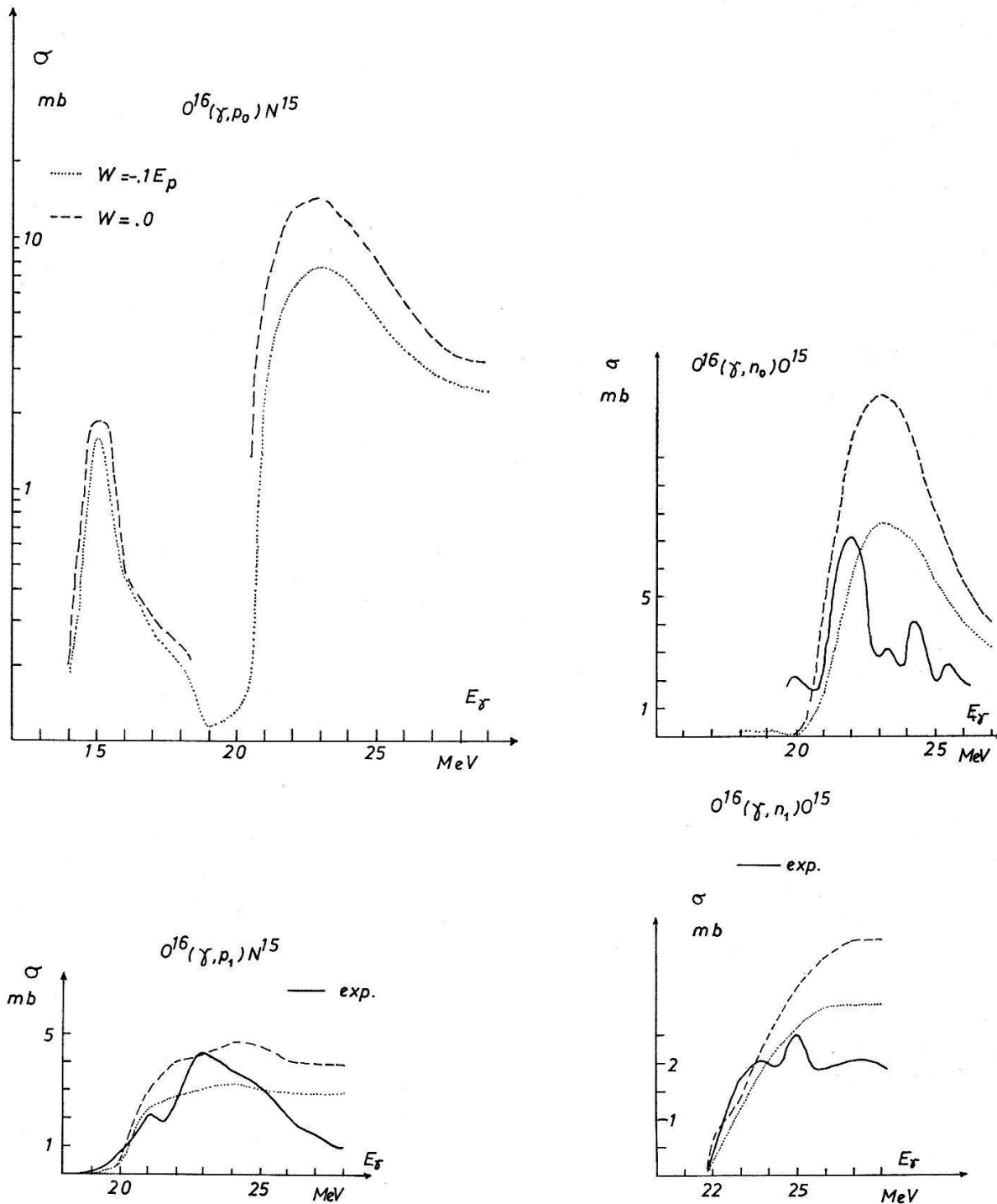


Figure 16

Total cross sections for  $O^{16} + \gamma$ -reactions. The experimental data were taken from Ref. [5]. The following parameter values were used in the calculations:  $V_0 = -55$  MeV,  $V_{1s} = -7.5$  MeV,  $R = 2.96$  fm,  $a_d = 0.5$  fm,  $V_p = -650$  MeVfm<sup>3</sup>,  $a = 0.7$ ,  $b = 0.3$  and for the absorption parameter  $W = -0.1 E_p$  and  $W = 0$ .

## 2. The Giant Resonance in $O^{16}$

For  $O^{16}$  we use again the spherical shell model. The ground state configuration is  $(1 s_{1/2})^2, (1 p_{3/2})^4, (1 p_{1/2})^2$  for both neutrons and protons. The giant-dipole state is formed by lifting nucleons from the  $1 p$  shell into the  $2 s, 1 d$  shell. The ground states of  $N^{15}$  and  $O^{15}$  are treated as pure one hole configurations  $(1 p_{1/2}^{-1})$ , and similarly the  $3/2^-$  excited states at 6.33 MeV in  $N^{15}$  and at 6.16 MeV in  $O^{15}$  are treated as

( $1 p_{3/2}^{-1}$ ) hole states. Only these states can occur in our model as final states of the photodisintegration. In Figure 18 the low lying levels of  $N^{15}$  and  $O^{15}$  are shown. The hole energies are extracted from the proton and neutron separation energies of  $O^{16}$  and the single particle spectra of  $O^{15}$  and  $N^{15}$ . We obtain a  $1 p_{1/2}$  hole energy of 12.11 MeV for protons and of 15.65 MeV for neutrons. For the  $p_{3/2}$  hole energy we obtain 18.44 MeV for protons and 21.81 MeV for neutrons.

For the hole wave functions harmonic oscillator wave functions have been assumed, which fulfill the condition  $\langle r^2 \rangle = 3/5 R^2$ . The Hartree-Fock potential is replaced again by a local optical potential given in equation (2.19). In principle, these potentials may be dependent on the nuclear state but in order to limit the number of parameters, they were chosen to be the same for all channels. The values  $V_0$ ,  $V_{1s}$ ,  $W$  are rather well known from other experiments, and were varied only to a small extent for a best fit to the experiments. The same procedure was applied to the strength  $V_p$  of the two particle interaction.

The  $1p-1h$  excitations occurring in the case of channel spin  $1^-$

$$(1 p_{3/2}^{-1} s_{1/2}), (1 p_{3/2}^{-1} d_{3/2}), (1 p_{3/2}^{-1} d_{5/2}), (1 p_{1/2}^{-1} s_{1/2}), (1 p_{1/2}^{-1} d_{3/2})$$

were coupled to states of isospin  $T = 0$  and  $T = 1$ . As discussed above, the Coulomb interaction was treated exactly in the external region by means of the matching procedure.

With the model described above we may calculate cross sections for the following 4 processes and their time reversed processes:

$$O^{16}(\gamma, p_0)N^{15}, O^{16}(\gamma, p)N_{6.33}^{15*} \text{ MeV}, O^{16}(\gamma, n_0)O^{15} \text{ and } O^{16}(\gamma, n)O_{6.16}^{15*} \text{ MeV} .$$

The cross sections for  $O^{16} + \gamma$  and for the reaction  $N^{15}(p, \gamma_0)O^{16}$  have been measured. Especially Caldwell [21] was able to measure the 4 processes separately. Also transitions to the positive parity levels in  $O^{15}$  and  $N^{15}$  occur, but Caldwell found the probability to be small. The 1-hole final states account for  $78 \pm 8\%$  of the total absorption cross section, in accordance with the  $1p-1h$  model. In order to explain transitions into the positive-parity levels one would have to extend the model at least to  $2p-2h$  excitations. As Caldwell's experiments have shown, however, these components are only weakly excited, so that we may neglect them here, although they seem to be responsible for the fine structure [22].

The calculations performed here do not show such a well developed fine structure as has been found in the various experiments, especially for  $N^{15}(p, \gamma_0)O^{16}$ . However, the absolute magnitude and position of the giant resonance are reproduced, as well as the angular distribution parameter  $a_2$ . The parameters used are practically fixed by other experiments and may be varied only very little, so that one actually does not use adjustable parameters. Obviously, the  $1p-1h$  model does not suffice to explain the fine structure and the (weak) transitions to the positive parity levels. Some calculations have been performed. If the parameters are changed we obtain the following results which correspond to those of  $C^{12}$ . A decrease of  $|V_p|$  moves the peak to lower energies and a decrease of  $|V_0|$  moves the peak to higher energies. The addition of an imaginary part in the optical potential lowers the cross section for all energies, especially in the region of the peaks. The imaginary part is important in obtaining the correct order of magnitude of the cross section (see Figure 16). The imaginary part in the potential roughly compensates for channels, which are not

treated explicitly in our model. The dominant channel is the  $N^{15}(p, \alpha)C^{12}$  reaction. For a qualitative understanding of the situation see below.

The measured angular distribution of the  $N^{15}(p, \gamma_0)O^{16}$  reaction has been expressed in the form of a Legendre polynomial expansion:

$$\frac{d\sigma}{d\Omega} = \frac{\sigma_{total}}{4\pi} \left( 1 + \sum_{\nu > 0} a_\nu P_\nu(\cos\vartheta) \right). \quad (4.13)$$

It was found that  $a_1, a_2, a_3 \neq 0$ . In Figure 17 we give a comparison between the experiments by Baglin and Thompson [23] and our calculations for pure E1-radiation for  $a_2$ . The model used here makes definite predictions for the intensities and phases of the partial waves. The phases vary rather quickly in the region of a resonance but slowly elsewhere. The resonance energies are at about 23 MeV for the  $d_{3/2}$ -level and at about 15 MeV for  $s_{1/2}$ .

Thus the energy region from 13–28 MeV can, roughly speaking, be divided into three different parts: First,  $E_\gamma > 24$  MeV, where the  $d_{3/2}$ -part is much more important than the  $s_{1/2}$  part. We obtain, therefore, for the angular distribution parameter  $a_2 = -0.5$ . Second, the region with  $15 \text{ MeV} < E_\gamma < 24$  MeV. Here the  $s_{1/2}$  part plays a role as well, contributing to  $a_2$  in the interference term  $-1/\sqrt{2} \text{Re}(x_{1/2} x_{3/2}^*)$ . The phase between  $x_{1/2}$  and  $x_{3/2}$  is of the order of  $\pi$ . We obtain, therefore, a positive contribution. Third,  $E_\gamma < 15$  MeV, where the  $s_{1/2}$  part dominates, so that the angular distribution becomes isotropic, i.e.  $a_2 = 0$ .

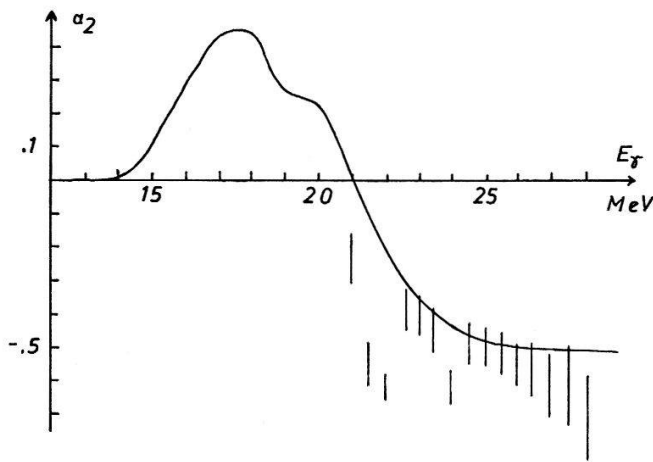


Figure 17  
The angular distribution parameter  $a_2$  for the reaction  $N^{15}(p, \gamma_0)O^{16}$ . The parameter set in Figure 16 is used. The experimental data were taken from Ref. [23].

Let us make some additional remarks on the dependence of the cross section on the relevant parameters.

The coupled channel equations are rather complicated, and it is difficult to deduce formally qualitative results for the solutions when the parameters are varied. However, one would expect to obtain the behaviour described above for physical reasons:

- (i) In a deeper potential well the resonance energies move to smaller energies.
- (ii) The influence of the two particle interaction is most readily studied qualitatively in the schematic model of Brown and Bolsterli [1]. It was shown there that an increase of the strength  $|V_p|$  of the two particle interaction moves the resonance peak to higher energies. Our numerical results lead to the same conclusion, although it is difficult to understand this qualitatively.

(iii) The absorptive part in the optical potential includes in an approximate way channels not treated explicitly. This leads to a lowering of the cross section, as has also been found numerically.

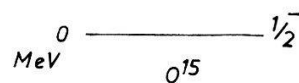
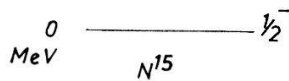
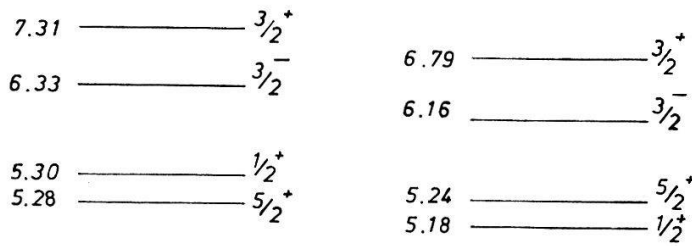


Figure 18  
Level schemes of  $N^{15}$  and  $O^{15}$ .

### Acknowledgments

One of the authors (G.B.) is grateful to the Swiss National Foundation for financial support. We thank dipl. phys. Th. Ballmer for help in the calculations. The numerical calculations were done on the UNIVAC 1108 of Sandoz AG, Basel.

### REFERENCES

- [1] G. E. BROWN and M. BOLSTERLI, Phys. Rev. Lett. *3*, 472 (1959).
- [2] H. STEINWEDEL, J. H. D. JENSEN, Z. Naturforsch. *5a*, 413 (1950).
- [3] M. KAMIMURA et al., Nucl. Phys. *A 95*, 129 (1967).
- [4] M. G. HUBER, H. J. WEBER, W. GREINER, Z. Physik *192*, 223 (1966).
- [5] B. BUCK and A. D. HILL, Nucl. Phys. *A 95*, 271 (1967).
- [6] N. VINH-MAU, Nucl. Phys. *54*, 321 (1964).
- [7] T. TAMURA, Rev. Mod. Phys. *37*, 679 (1965).
- [8] Nucl. Data *1 A*, 21 (1965/66).
- [9] TH. BALLMER, private communication (Diplomarbeit).
- [10] A. R. EDMONDS, *Drehimpulse in der Quantenmechanik* (Hochschultaschenbücher-Verlag, Mannheim 1964).
- [11] M. MARANGONI, A. M. SARUIS, Phys. Lett. *24 B*, 218 (1967).
- [12] D. ROBSON, Phys. Rev. *137 B*, 535 (1965).
- [13] C. MAHAUX and H. A. WEIDENMÜLLER, *Shell-Model Approach to Nuclear Reactions* (North-Holland Publ., Co., Amsterdam 1969), p. 278.
- [14] N. VINH-MAU, G. E. BROWN, Nucl. Phys. *29*, 89 (1962).
- [15] D. DREHSEL, J. B. SEABORN and W. GREINER, Phys. Rev. *162*, 983 (1967).
- [16] S. PENNER and J. E. LEISS, Phys. Rev. *114*, 1101 (1959).
- [17] D. S. DOLBILKIN, *Photodisintegration of Nuclei in the Giant Resonance Region*, ed. D. V. Skobel'tsyn (Consultants Bureau, New York 1967), p. 68.
- [18] D. E. FREDERICK, A. D. SHERICK, Phys. Rev. *176*, 1177 (1968).
- [19] R. G. ALLAS, S. S. HANNA, L. MAYER-SCHÜTZMEISTER and R. G. SEGEL, Nucl. Phys. *58*, 122 (1964).
- [20] M. M. BLATT, V. F. WEISSKOPF, *Theoretical Nuclear Physics* (John Wiley, New York 1952).
- [21] J. T. CALDWELL, Phys. Rev. Lett. *19*, 447 (1967).
- [22] V. GILLET et al., Nucl. Phys. *A 97*, 631 (1967).
- [23] J. E. E. BAGLIN and M. N. THOMPSON, Nucl. Phys. *A 138*, 73 (1969).